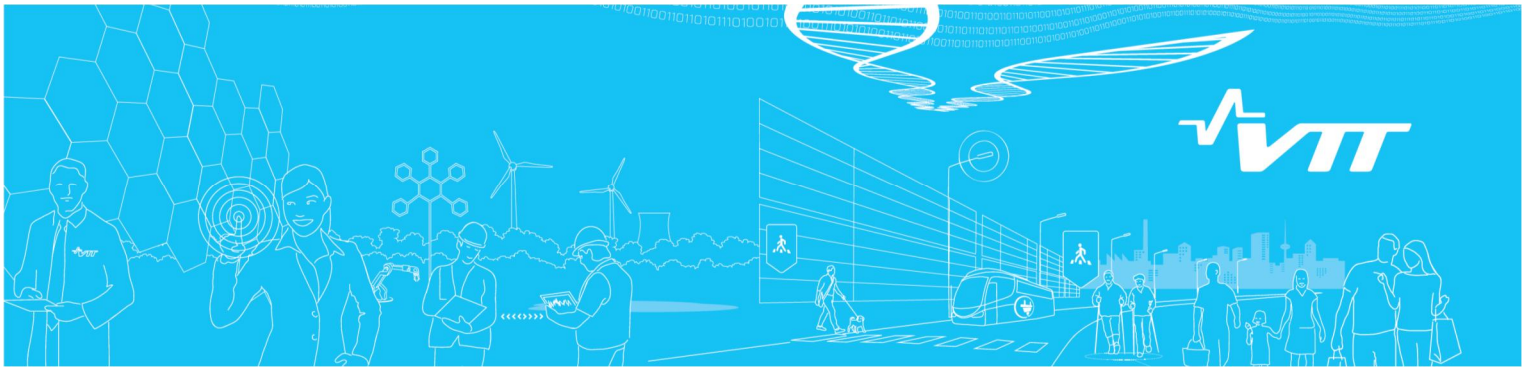

RESEARCH REPORT-+

VTT-R-02327-17

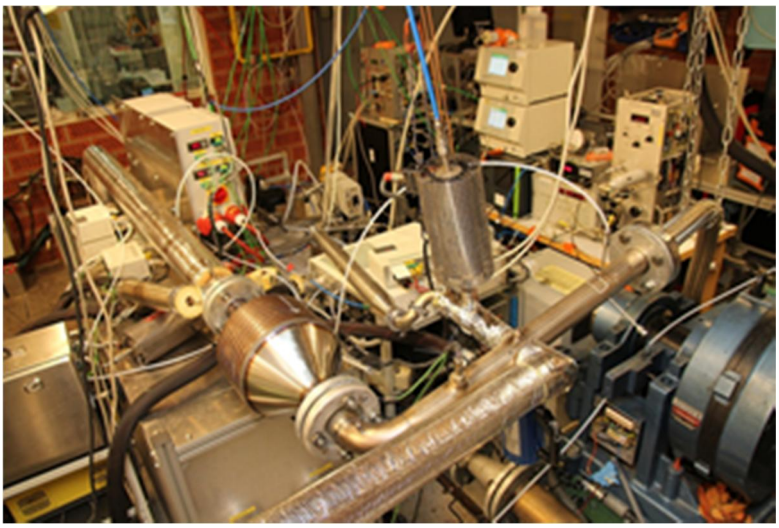

Controlling emissions of natural gas engines – Final report

Authors: Kati Lehtoranta, Timo Murtonen, Hannu Vesala, Päivi Koponen
VTT Technical Research Centre of Finland

Jenni Alanen, Topi Rönkkö, Pauli Simonen
Tampere University of Technology

Sanna Saarikoski, Hilkka Timonen
Finnish Meteorological Institute

Confidentiality: {Public}

Report's title Controlling emissions of natural gas engines – Final report	
Customer, contact person, address	**Order reference**
Project name Controlling emissions of natural gas engines	**Project number/Short name** CENGE
Author(s) Lehtoranta et al.	**Pages** 60
Keywords	**Report identification code** VTT-R -02327-17

Summary

The CENGE project focuses on characterization of gas engine emissions comprehensively and studies the effect of different techniques on the emission formation. In addition different emission measurement methods are studied. To mimic the emission matrix of 4 stroke medium speed gas engine a new test facility is developed. The project is based on experiments conducted in engine laboratory and on power plant.

Measurements of natural gas engine exhaust gas emissions resulted to rather high levels of hydrocarbons and carbon monoxide. The main HC component was methane while ethane, propane and ethylene were also found. These components are found also in the natural gas. The NO_x and particle mass emissions were low. However, significant amount of nanoparticles was found in the exhaust.

Several different catalysts were studied, including SCRs, oxidation catalysts, a methane oxidation catalyst (still under development) and combinations of those. High NO_x reductions were observed when using selective catalytic reduction, although a clear decrease in the NO_x reduction was recorded at higher temperatures. The relatively fresh methane oxidation catalyst was found to reach reductions greater than 50% when the exhaust temperature and the catalyst size were sufficient. At all measurement campaigns catalysts were found to decrease the emissions of particulate matter total mass. However, nanoparticle number concentrations were increased by a catalyst combined with high exhaust temperatures. In one experiment, the behaviour was connected to sulphur compounds while in the other, by contrast, the increase in particle emission at higher catalyst temperatures was due to an increase in organics. The engine out particle emissions between these measurements differed also, one explanation to this being the change of lubricating oil.

In addition to primary particle emissions, secondary emission was studied utilizing a potential aerosol mass (PAM) chamber: the particle mass measured downstream the PAM chamber, was found to be 6-170 times as high as the mass of the emitted primary exhaust particles. The fraction of organics was approximately half of the produced secondary aerosol mass.

Confidentiality	Public

Espoo 28.4.2017

Written by	**Reviewed by**	**Accepted by**
Kati Lehtoranta, Senior Scientist	Timo Murtonen, Senior Scientist	Jukka Lehtomäki, Research Team Leader

VTT's contact address
P.O.Box 1000, FI-02044 VTT

Distribution (customer and VTT)

CENGE project partners and Tekes, in addition distribution through VTT's publication database.

Contents

Introduction

Trends affecting engine development and energy production are global; e.g. due to the global warming several political actions have been conducted to decrease CO_2 emissions and, due to the air quality problems and health effects of combustion emissions, the emissions have been restricted by stricter emission limits practically in all countries. At the same time the crude oil reserves are diminishing causing higher production costs for liquid fossil fuels. The opposite trend can be seen in the production and use of natural gas; due to the production technology development (extraction of shale gas) the NG production has increased and both the availability and the delivery reliability have enhanced (e.g. new natural gas pipe from Russia to Central Europe, increase of shale gas production in US and Europe). It seems that this development will continue in near future.

Natural gas (NG) is a promising alternative fuel from many different perspectives (see Figure 1): its availability increases, and its use leads to lower CO_2 emissions compared to conventional liquid fossil fuels. Lower emissions are due to chemical properties of NG with high H/C ratio, as natural gas is primarily composed of methane (e.g. Cho and He 2007). When compared to e.g. diesel engines with NG engines lower levels of NO_x can be achieved at lean burn conditions while the CO and HC emissions have a tendency to increase at those conditions. Several studies have shown that NG engines have higher CO and HC emissions compared with liquid fuel engines (e.g. diesel engines) (e.g. Cho & He 2007, Hesterberg et al. 2008, Abdelaal & Hegab 2012, Liu et al. 2013). The HC and VOC (volatile organic compounds) are recognized to have environmental as well as health effects. E.g. the VOCs are involved in stratospheric ozone depletion as well as in ground level ozone formation. One emission component that is relevant especially in NG engines is formaldehyde. Formaldehyde is a toxic emission. Formaldehyde can be emitted from NG engines as a product of incomplete combustion, mostly due to partial oxidation events in the engine (Olsen et al. 2000, Mitchell et al. 2000).

PM (mass) emissions from NG engines are known to be low e.g. when compared to conventional diesel engines. This is because of lower soot particle formation in combustion. Thus, the larger use of NG engines can lead to benefits for human health and climate. However, recent studies indicate that particle number emissions of NG engines, especially nanoparticle emissions are not necessarily low (e.g. Jayaratne et al. 2009). Particles can affect the climate as well as health. Especially the smallest particles (nanoparticles) can penetrate into the lungs and blood-vascular system (e.g. Pope & Dockery 2006). Also, especially the nanoparticle emissions might be more sensitive on technology changes and e.g. engine parameters than soot particles. In general, only few studies have been focused on NG combustion particle emissions and their detailed characterization and thus there are many open questions related to those.

Although it seems clear that NG engines are less harmful to the environment than e.g. conventional diesel engines, they still need techniques to reduce emissions. The regulated emission components are rather well known but in order to affect the emission formation process, more specific emission characterization is needed. It also seems that most of the NG emission studies so far are done in vehicle applications. The results of those are not directly comparable to medium speed (stationary, ship) engines as e.g. the engine technique, fuel injection and ignition are not all similar when comparing vehicle and medium speed engines.

There are many regulations (country, federal and regional regulations) for emissions of stationary engines used in energy production. The future regulations drive the emission levels even lower. Therefore e.g. although NG engine can achieve low engine out NO_x emissions the use of deNO_x system, like selective catalytic reduction (SCR), might be needed to meet the most stringent emission regulations. Also, oxidation catalysts are being developed in order to remove CO and hydrocarbons. Catalysts may also, unintentionally,

affect other emissions components, including particle composition. Depending on the application, combinations of different catalyst systems might be needed.

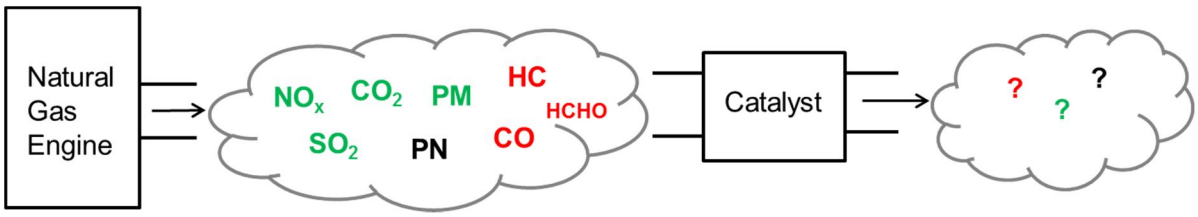

Figure 1Expected emissions from NG engine (red indicates high levels, green low levels, black can be either).

In this project we conducted comprehensive gaseous and particle emissions studies for NG engine exhaust and studied how the catalyst systems affect the exhaust gas composition utilizing several measurement methods and instruments. The work started with a development of a new research facility to mimic the real application medium speed gas engine exhaust matrix in laboratory (Task 1). Gaseous and particle emission studies were done both on the new facility as well as on a real application engine (Tasks 2-4). Effects of different catalysts, relevant to be utilized in gas engine applications, were studied by emission measurements upstream and downstream of the catalyst(s) (Task 3). Several measurement methods and instruments, both newly developed and well known, were utilized in the measurements of this project (Tasks 1-5).

Project partners were: VTT Technical Research Centre of Finland, Tampere University of Technology and Finnish Meteorological Institute. In addition, company partners were AGCO Power, Dekati, Dinex Ecocat, Neste, Suomi Analytics and Wärtsilä.

Project Target

The project objectives were:

- To develop novel research infrastructure for NG emission studies including NG research engine and sophisticated test bench for after-treatment systems
- To conduct comprehensive emission studies for NG engine
- To study effects of new catalysts on emissions
- To develop, test and compare emission measurement methods and instruments

A research infrastructure to study the natural gas engine emissions in detail and to develop after-treatment and measurement techniques was build up. Typically, catalysts are developed in small scale in laboratory with synthetic gases without using a real exhaust gas. The results with synthetic gas need to be confirmed with real exhaust gas and in vehicle size class this can be easily done with real engine or vehicle. On the contrary, in applications related to larger engines (stationary power plants and ships) the testing can be challenging and expensive. Large engines require large catalyst volumes to deal with the emissions. Installations to large engine applications can be challenging and testing rather complex. Only minor tuning of the parameters is possible in real applications. Therefore a novel research infrastructure with small NG engine and catalyst test bench was needed.

Using the novel research infrastructure the emissions of NG engine with and without exhaust after-treatment system were characterised thoroughly. The exhaust gas composition was adjusted to mimic real life applications and regulated and unregulated emissions were measured and analysed. The effect of temperature and flow rate was studied without changing the exhaust gas composition.

The results of the emissions measurements can vary a lot depending on the measurement methods. For instance, the measurement of formaldehyde can be done by analysing from samples collected using dinitrophenyl-hydrazine (DNPH) cartridges but also with FTIR (on-line measurement) leading possibly to two different results. Particle emission is not easy to define either; e.g. in PM measurements the amount of absorbed and condensed matter strongly depends on the cooling and dilution conditions of exhaust sample. Therefore in this study different particle emission measurement methods were studied and compared. In general, it is important to understand the differences of analysis and measurement methods to evaluate results gained with different methods.

Task 1 - Natural gas engine research facility

Target: To develop novel research infrastructure for NG emission studies including NG research engine and sophisticated test bench for after-treatment systems

Test engine

A 2.0 litre naturally aspirated Mercedes Benz gasoline engine (model MB111) converted to run on NG was used for mimicking the exhaust gas emissions of a four stroke medium speed stationary NG engine. The engine was connected to a Zöllner B-300 AD eddy-current dynamometer. For the NG usage, a parallel fuel injection system was installed on the engine, and the original engine control unit (ECU) was replaced with an aftermarket ECU which could be re-programmed for research purposes.

The fuel injection system for NG included four fuel injectors installed in the cylinder specific ducts of the intake manifold. The injectors were operated sequentially in pairs like the original fuel injectors. A fuel gas pressure regulator was part of the system for maintaining the constant gas pressure at the fuel injectors. For the NG usage, the original ignition system was also replaced with a more powerful system, which was needed for operation with a lean air-to-fuel mixture.

Table 1 Test engine specifications.

Engine model	111.940
Engine type	In-line, 4-cylinder, naturally aspired
Displacement	1998 cm3
Power	100 kW / 5500 min-1
Torque	190 Nm / 4000 min-1
Fuel injection	multi-point injection
Ignition	Bosch Double-Fire Coil
ECU	Hestec 32

The aftermarket ECU (Hestec 32) was used to control the engine parameters such as injection and ignition timing and air-to-fuel ratio (AFR). The ECU has separate fuel maps for gasoline and natural gas usage. It also has closed-loop control systems to control the AFR. In this study, the NO_x-sensor signal was used for the closed-loop control system and the engine was driven in “closed-loop NO_x control mode”.

The closed-loop NO_x control mode was used since the stability of NO_x concentration was essential to this study. The NOx emission of a small naturally aspired and spark-ignited engine is sensitive to changes in test bed atmospheric pressure, humidity and temperature. The test cell temperature was kept constant with a controlled cooling system, but the test cell pressure and humidity were not controlled. Without an accurate engine control system, the NO_x emissions would have varied too much due to changes in pressure and humidity conditions. Basically, the ECU adjusted air-to-fuel ratio (AFR) to maintain the correct NO_x level. The needed adjustments to AFR were moderate and the effect of adjustment on the other emission compounds was negligible in this case. Two Continental UniNO_x sensors were utilized for monitoring NOx levels up- and downstream of the after-treatment system (see figure 2).

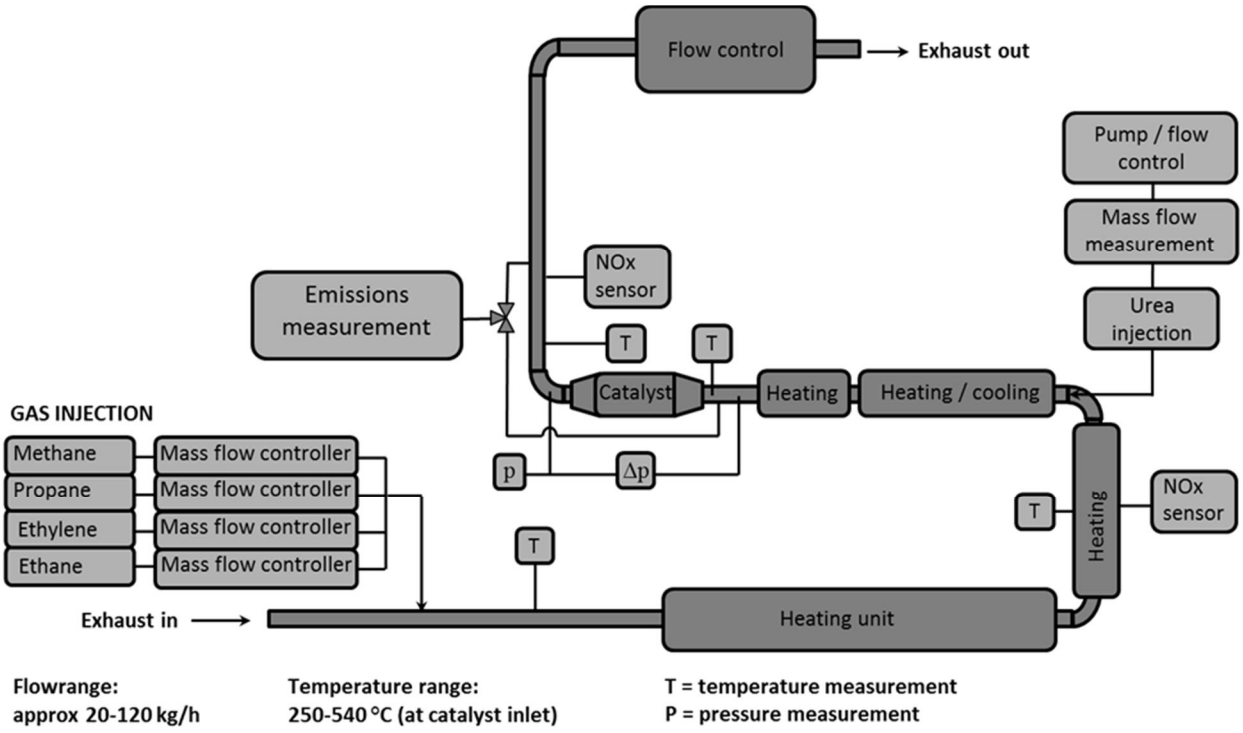

Figure 2 Research facility.

Results

The reference values (see Figure 3) represent an estimation of a large NG engine emission matrix. In real life applications, the engine emissions depend on engine technology, how the engine is tuned for the specific application and the composition of the fuel gas used. The selected reference values covered four different exhaust gas matrixes (mode 1…mode 4). In the laboratory, three different engine operating points together with HC compound additions were used to mimic these modes. The selected engine operation modes were compromises between different emission compounds. In mode 1, the desired emission matrix was achieved without any gas additions. In mode 2, methane was added to the exhaust gas, and in modes 3 and 4, the added compounds were methane, ethane, propane and ethylene.

The emission concentrations in selected driving modes met the reference values quite well. The emission measurement setup and the measurement devices are presented in task 2.

With NO_x emissions, the difference between reference and measured values ranged from 0 to 30%. The highest difference was in mode 3. The measured CO emissions were within -3 to 13% in modes 1–3 and -23% in mode 4 compared to reference values. THC concentrations measured with HFID were from -19% to 33% compared to reference values. The highest difference (33%) was in mode 1. Though the percentage differences are in some cases relatively high, the overall correspondence between measured and reference values were considered to be acceptable for mimicking the emissions of a power plant size class engine.

The Figure 3 also presents the measured formaldehyde concentration compared to reference values. The aldehyde emissions were analysed with HPLC method, and the only detected aldehyde compound was formaldehyde. The formaldehyde values with VTT's engine were quite insensitive to different operating modes. The formaldehyde concentrations measured ranged from 49 to 62 ppm while the corresponding reference values were in-between 34 and 118 ppm. The difference between measured and reference values was

highest in mode 4. The level of formaldehyde in the exhaust cannot be fine-tuned by gas injection as with the hydrocarbons due to the physical characteristics of formaldehyde.

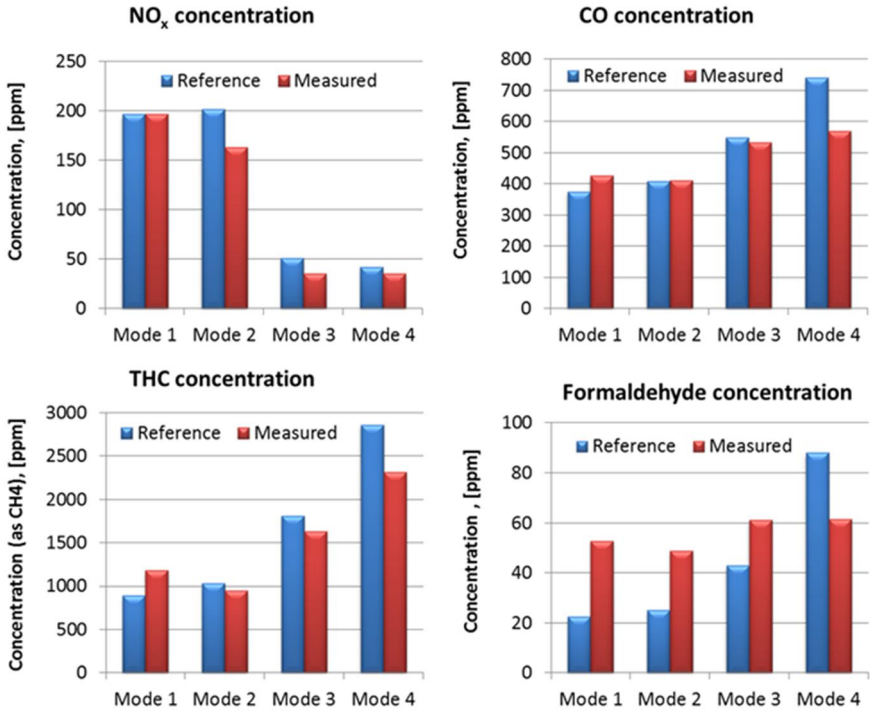

Figure 3 Measured NO_x, CO, THC and formaldehyde emissions compared to reference values (Murtonen et al. 2016).

The standard deviation of the measurement results was not reasonable enough in the first measurements. Therefore modifications were done, including updating both the engine control system and ignition system. As a result a return coupling from NO_x sensors was possible. This way, also the effect of environmental parameters (atmospheric pressure and relative humidity) to the emissions results (especially NO_x results) was minimized. The much more stable performance can be seen from the NO_x levels measured after these modifications (in Figure 4).

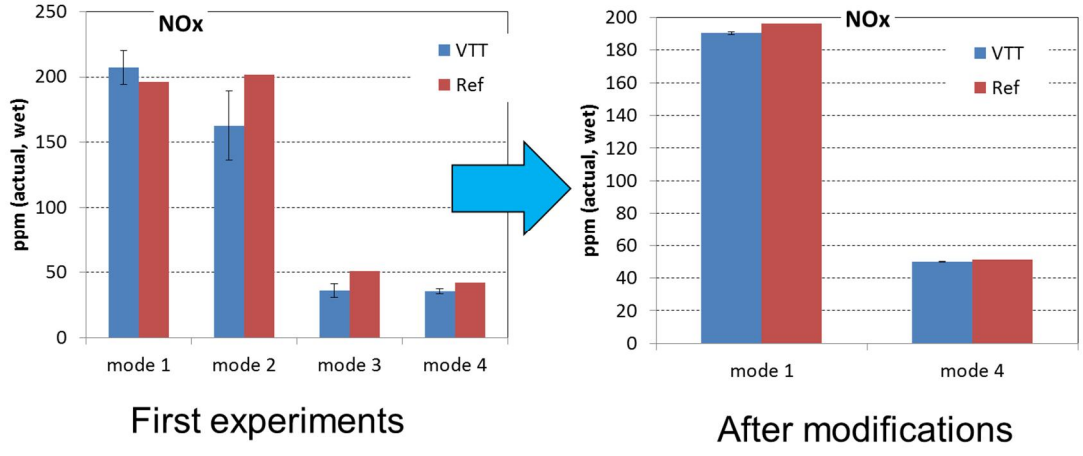

Figure 4The NO_x emissions (ppm). The error bars show the standard deviation.

Main findings of task 1

As a result of task 1 a unique research facility has been developed. By this research facility the emission matrix of a power plant NG engine can be mimicked. The emission comparisons (research facility versus power plant engine) are very promising.

In this CENGE project and in the related company projects the research facility has been successfully utilized for over 2000 hours of running.

The research facility has been presented in CIMAC conference 2016: Murtonen T., Lehtoranta K., Korhonen S., Vesala H., Koponen P. Test facility for catalyst studies utilizing small NG engine. CIMAC Paper 107, 2016.

Task 2 - Emissions characterization

Target: To conduct comprehensive emission studies for NG engine

In task 2 the first extensive experimental emission characterization was done together with all the research partners (VTT, TUT, FMI). This covered both gaseous and particle emissions measurements in different driving modes.

The emissions are formed as a result of an incomplete combustion process. In addition to the combustion process (e.g. engine technique) the fuel is in key role in the emission formation. In this case the fuel is natural gas. Natural gas from the Nord Stream pipeline has high methane content. In the present study, the gas analysis results were: 97.2 % methane, 1.37 % ethane, 0.17 % propane, 0.07% other hydrocarbons, 0.9 % nitrogen and 0.2 % carbon dioxide. The sulphur content of the gas was below 1.5 ppm according to Gasum.

When the emissions are low the effect of lubricating oil on the emission formation usually increases. Two different lubricating oils were utilized in this task. The lubricating oil sulphur contents were 1760 and 1282 mg/kg, for oil 1 and oil 2, respectively. The density was 852.5kg/m^3 and the viscosity at 100ºC was 12.0 mm^2/s and these were the same for both oils (see more about the lube oils in appendix).

Emission measurement setup

The gaseous emission measurement setup consisted of a chemiluminescence detector (CLD), used to measure the NO_x (NO, NO_2), a non-dispersive infrared (NDIR) analyser to measure CO and CO_2, and paramagnetic method for O_2 Horiba PG-250 analyser and Ecophysics 700 ELht heated chemiluminescence analyser (HCLD) were utilized. A J.U.M HFID 109A analyser was used for measuring THC and methane concentrations.

Gasmet DX-4000 fourier transformation infrared (FTIR) was used for measuring multiple gaseous compounds (e.g. water, methane, formaldehyde). The FTIR as well as the sampling line and the filter prior to the FTIR spectrometer were heated to 180 °C. In addition, methane, ethane, propane and ethylene components were measured from a diluted exhaust gas sample with a gas chromatograph (GC). Hewlett Packard 5890A Series II gas chromatograph (GC) was used and the diluted exhaust gas samples for the gas chromatograph were collected in Tedlar® bags.

Aldehyde samples were collected from diluted exhaust gas by using the DNPH (dinitrophenyl hydrazine) cartridges. In the cartridges, aldehydes form hydrazine derivatives which are then analysed by high performance liquid chromatography. The DNPH derivatives were extracted with an acetonitrile, and the extraction was diluted with water (1:1) and analysed with the HPLC-technology (Agilent 1260, UV detector, Nova-Pak C18 column).

The sample for GC and aldehyde measurement was taken from the FTIR output, utilizing a T-branch diluter and a tracer (Sulphur hexafluoride, SF_6) to define the exact dilution ratio. The target dilution ratio was 10, and it was determined with FTIR using sulphur hexafluoride (SF6) as a marker gas in dilution media (N_2). In practice the dilution ratio was observed to be 9-13.

Particulate matter (PM) was measured with a sampling according to international standard ISO 8178-1:2006. According to this standard the PM is measured as any material collected on a filter after diluting exhaust gas with clean, filtered air to a temperature higher than 42 °C and less than or equal to 52 °C, as measured at a point immediately upstream of the filter. A dilution ratio of 10 and a sampling time of 30 minutes were used. Samples were collected on TX40HI20-WW filters.

Another particle emission sampling system consisted of a porous tube diluter (PTD), a residence time tunnel and an ejector diluter (Dekati Ltd). Sample was taken from the exhaust pipe after an exhaust gas heating unit to dilution system. Residence time in the primary dilution system, i.e. in the PTD and the residence time tunnel, was 2.6 s. The dilution ratio over the porous tube diluter during the measurements was set to be as small as 6 because the particle concentrations in exhaust line were low and close to detection limit of used aerosol instruments. The secondary dilution ratio over the ejector diluter was 4.

Particle size distribution and number concentration were measured using three instruments that together covered a wide particle mobility size range. A particle size magnifier (PSM, Airmodus Inc.) together with a condensation particle counter (CPC 3775, TSI Inc.) was used to measure size range 1.7-7.2 nm. A scanning mobility particle sizer equipped with DMA 3085 and UCPC 3025 (TSI Inc.) was used in size range 3-60 nm (Nano-SMPS). The sample flow was 1.5 lpm and sheath flow 15 lpm. An engine exhaust particle sizer (EEPS, TSI Inc.) was used to cover size range 5.6-560 nm. EEPS default inversion matrix was applied. UCPC 3776 (TSI Inc.) was measuring beside PSM and its purpose of use was to monitor changes and support PSM total concentration data.

Thermodenuder (TD) and Nano-SMPS neutralizer could be bypassed. The extra dilution before EEPS was organized using a HEPA filter and TSI Mass Flowmeter. The sample coming to PSM and UCPC was diluted with a dilution ratio (DR) 36. The particle losses of the diluter depended on particle size and the penetration curve was

$$\eta = 0.819exp(3.657\xi) + 0.097exp(22.3\xi) + 0.032exp(57\xi) \quad (1)$$

where $\xi = \pi DQL$ and D is diffusion constant of a particle, Q is flow rate through the diluter and L is the length 10.22 cm that the diluter corresponds based on fitting made on measurement data.

A thermodenuder at 265 °C was used to study particle volatility characteristics. Thermodenuder consists of a heated metal tube followed by an active charcoal that absorbs the evaporated compounds. The used thermodenuder is designed for ultrafine particle measurements.

Nano-SMPS was used without the neutralizer (Ion-SMPS) to study the electric charge state of particles. When Nano-SMPS is used without neutralizer, particles will be classified based on their existing charge state. The electric charge of particles was investigated by comparing the particle size distributions measured by Nano-SPMS and Ion-SMPS.

The emissions of CO_2 were measured from the diluted exhaust by Sick Maihak SIDOR gas analyser. CO_2 was used for defining the dilution ratios over both dilution systems. The SIDOR analyser was calibrated before the measurement campaign.

The chemical composition of the particles was measured using a soot particle aerosol mass spectrometer (SP-AMS, Aerodyne Research Inc., USA). SP-AMS is a combination of two instruments: an Aerodyne high-resolution time-of-flight aerosol mass spectrometer and a single-particle soot photometer (SP2; Droplet Measurement Technologies, CO, USA), and it is capable of measuring refractory and non-refractory particulate materials.

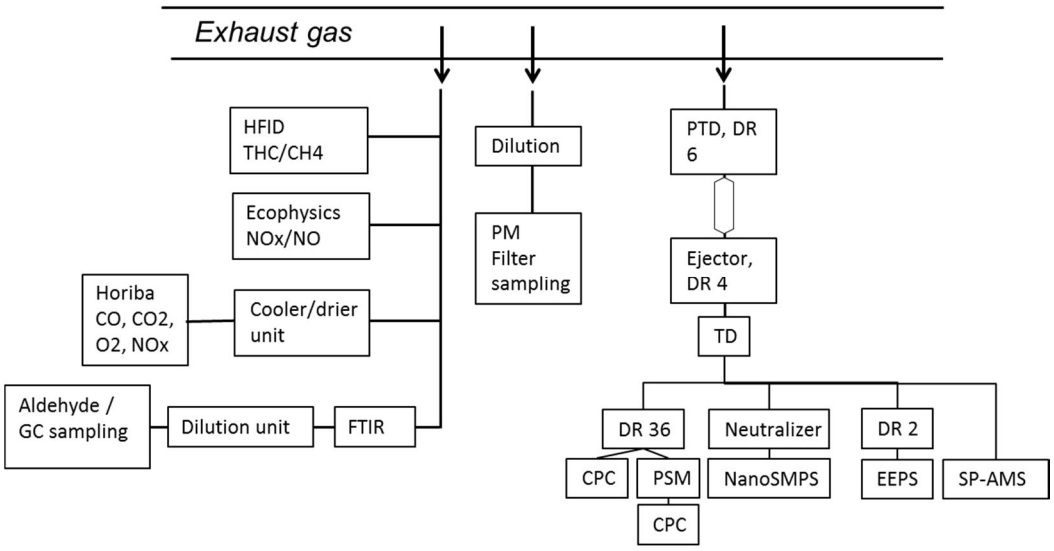

Figure 5 Measurement setup.

Gaseous emissions

The measured NO_x, CO, THC and formaldehyde levels were already presented in Fig. 3. The NO and NO_2 (resulting to NO_x) were measured with FTIR. Results reveal that the NO_2 level is significant (see figure 6). In good correlation with present results significant fractions of NO_2 has earlier been reported for the natural gas engines (e.g. Olsen et al. 2010, Ristovski et al. 2000).

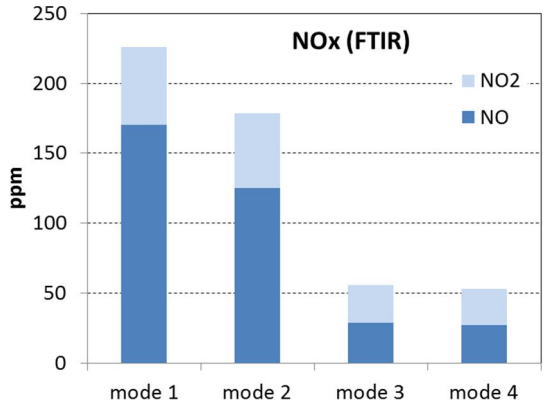

Figure 6 NO and NO_2 measured with FTIR.

Gas chromatography results revealed the main hydrocarbon components present in the NG engine exhaust gas. Methane was the main HC component in the exhaust gas as it is the main component also in the natural gas itself. In addition, ethane, propane and ethylene were also found in the exhaust. On should also keep in mind that these HC components were intentionally added to the exhaust gas (in some measurement modes) to achieve the levels near the case for a power plant natural gas engine exhaust. In mode 1, the desired emission matrix was achieved without any gas additions. In mode 2, methane was added to the exhaust gas, and in modes 3 and 4, the added compounds were methane, ethane, propane and ethylene.

For methane measurement, in addition to GC, also FID and FTIR were utilized. As seen in Figure 7, the results from different instruments are very near each other's in the methane level near 1000 ppm. However at the higher methane level near 2000ppm the FTIR gives

lower methane values. The reason for this was found to be in the FTIR references which cover only up to 1000ppm. For future measurements new references are needed.

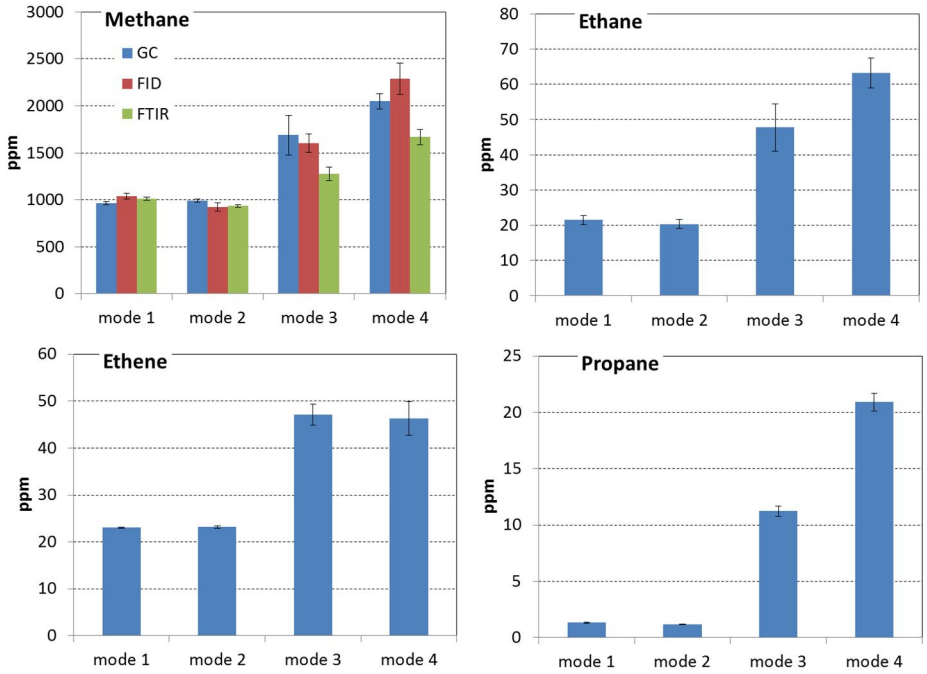

Figure 7 HC components measured with GC. Methane measured also with FID and FTIR (note. in FTIR references for methane only up to 1000ppm, this is the reason for underestimations at higher methane levels).

Aldehydes were measured with DNPH cartridges and also with FTIR. In practice, only formaldehyde was detected in measurable levels. The acetaldehyde and acrolein were found to be below 1 ppm in all tested driving modes.

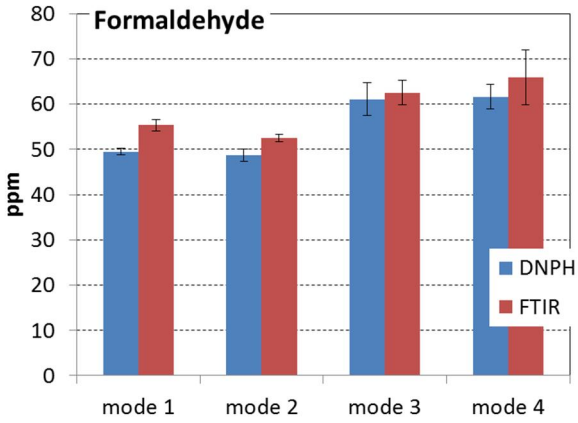

Figure 8 Formaldehyde results measured with DNPH cartridges and FTIR.

Particle emissions

The PM mass emissions were found to be at low level. However, the standard deviation was rather large (Figure 9). This might reflect the engine operation to be unstable and/or the sampling conditions (e.g. temperature) to be critical in the PM formation. Both, the engine control (done in Task 1) and the sampling temperature control were modified prior to next experiments in task 3.

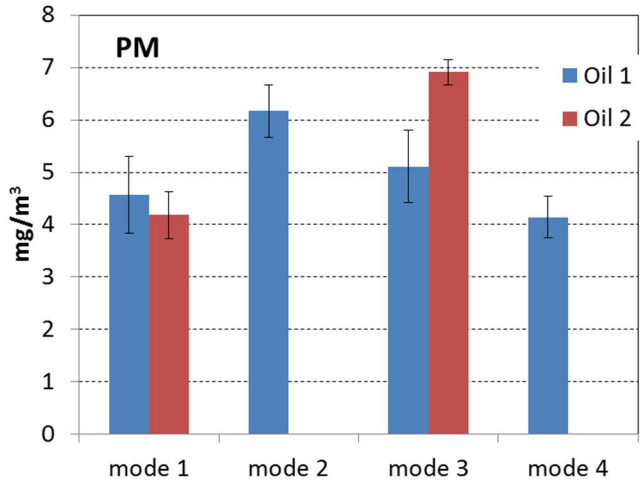

Figure 9 PM measured according to ISO 8178.

No clear differences were found in the gaseous emissions when comparing the results from the driving modes 1 and 3 studied with two different lubricating oils. The PM results are collected in Figure 9 and indicate that in driving mode 3 the change of lube oil affects the PM formation. However the standard deviation is rather large and it's difficult to draw any final conclusions according to this measurement. But due to this indication, in the future tests the effect of lube oil should be studied further.

Particles emitted from the natural gas engine were extremely small with the particle size distribution peak at about 2-5 nm. Another particle mode peak with much smaller number concentration was detected at particle sizes 6-10 nm (Figure 10). Number of particles with a diameter larger than 23 nm was low compared to particles with smaller diameter; less than 1% of the particles in the particle size range above 23 nm. Similarly to observations in the literature, the standard deviation of especially PSM size distribution concentrations was large.

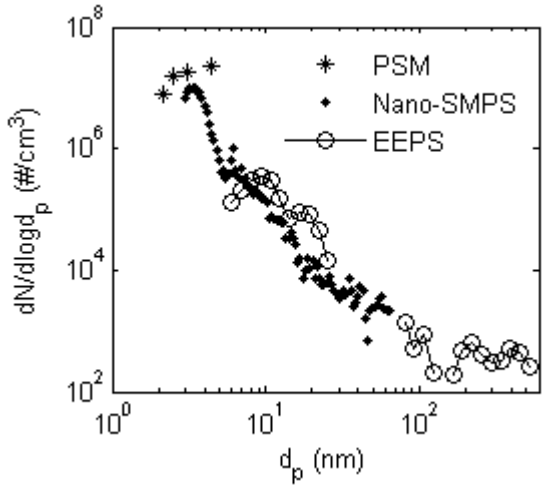

Figure 10 Particle number size distribution.

The concentration of the particles in the diluted exhaust, corrected by dilution factor, varied between $3 \cdot 10^6$ - $35 \cdot 10^6$ 1/cm^3 depending on engine test mode. Number concentrations were measured using PSM with saturator flow 1 l/min. The emission factors were calculated using information about engine power and combustion air consumption, and assuming the density of exhaust gas to be equivalent to that of air and combustion of the natural gas to be ideal.

Taking into account that all particles with diameter above ~1.5 nm were counted and the dilution conditions favored generation and growth of particles, the observed particle number concentrations were fairly small. In addition, the engine was run at unusually low loads because of the aim to produce gaseous emissions similar to those of a natural gas engine power plant.

The particle size shifted towards smaller sizes when sample was heated to 265 °C (Figure 11). When the torque of test engine was 34 Nm (imitated engine load 50%, mode 3) the shift of the particle size distribution peak was from ~4.5 nm to below 2 nm. The second particle mode shifted from ~9 nm to ~6 nm.

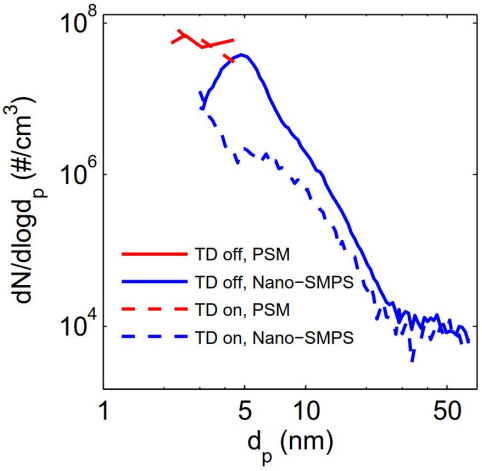

Figure 11 Shift of particle number distribution when the sample was heated in the thermodenuder

The physical properties of the particle were also measured. The strongest evaporation took place at temperatures from 50 to 120 °C (Figure 12) and approximately 40% of total volume remained at 265 °C (Figure 12). Electric charge of the particles was measured by Nano-SMPS (with neutralizer) and Ion-SMPS (without neutralizer) and comparing them with each other. It was observed that the concentration of particles measured by Ion-SMPS (particles unneutralized) was approximately three times higher than that measured by Nano-SMPS i.e. the particles carry approximately three times more positive electric charge than at equilibrium at room temperature. That would suggest that the particles have been generated in a higher temperature than room temperature. The Ion-SMPS and Nano-SMPS distributions displayed similar modal characteristics, indicating that the charging process of particles has been independent of particle mode. This result indicates that all the particles have been generated in a similar way.

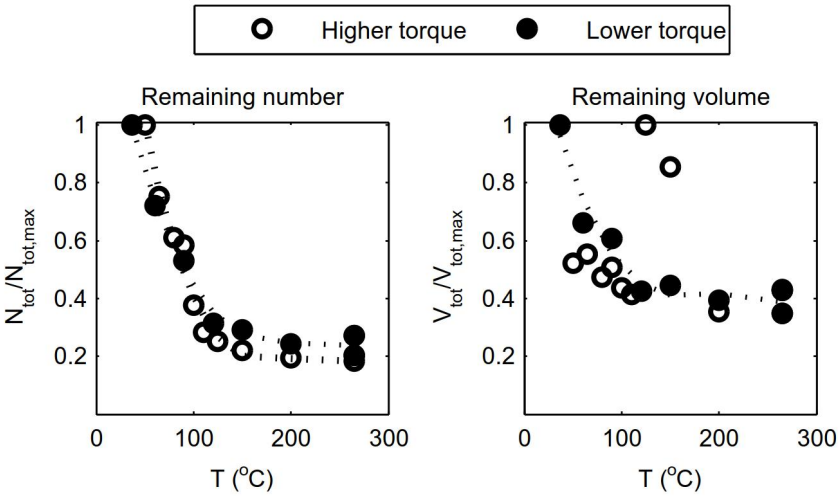

Figure 12 Remaining particle number and volume when sample was heated in the thermodenuder

It was concluded, that the origin of at least some particles was the engine cylinder or its vicinity (Figure 13). Natural gas and lubricating oil originated hydrocarbons and sulphur compounds could magnify the already existing particles in dilution and cooling process, where also new particle formation could happen.

Most of the results presented here are also published in Alanen et al. 2015.

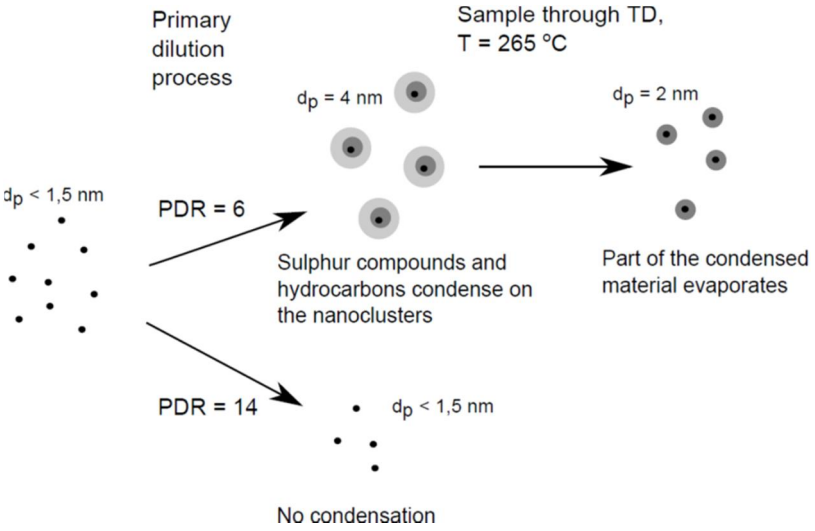

Figure 13. A suggested formation process for the natural gas engine exhaust particles.

Main findings of task 2

A comprehensive emission characterization of NG engine was done. The measured gaseous emissions results of NO_x revealed significant fractions of NO_2 while the NO was the main component of NO_x. Methane levels were measured with three different devices and the correlation was found to be very good. PM level was found to be low. In one measurement mode the change of lubricating oil indicates it might have an influence on the PM formation.

Particle size measurements showed that the particles emitted from the natural gas engine were extremely small with the particle size distribution peak at about 2-5 nm. Adding the volatility and electric charge measurement results a conclusion of the particle formation

process can be made: Particle emissions from natural gas engines form already in (or near) the combustion chamber, not only in the dilution and cooling process by nucleation.

Publications related to task 2:

Alanen J. Kaasumoottorin pakokaasun pienhiukkasten fysikaaliset ominaisuudet. Diplomityö 2014

Alanen, J.; Saukko, E.; Lehtoranta, K.; Murtonen, T.; Timonen, H.; Hillamo, R.; Karjalainen, P.; Kuuluvainen, H.; Harra, J.; Keskinen, J.; Rönkkö, T. The formation and physical properties of the particle emissions from a natural gas engine. Fuel 2015, 162, 155-161.

Alanen J., Saukko E., Lehtoranta K., Timonen H., Keskinen J. and Rönkkö T. 'Characteristics and formation of natural gas engine exhaust nanoparticles' Aerosol Technology 2015 June 15th to 17th, Tampere.

Murtonen T., Lehtoranta K., Korhonen S., Vesala H., Koponen P. Test facility for catalyst studies utilizing small NG engine. CIMAC Paper 107, 2016.

Task 3 - Catalysts studies

Target: To study effects of new catalysts on emissions

In this task, two different measurement campaigns were conducted. The first one is discussed in more detail in this chapter while only the new findings of second campaign are presented here. Some of the findings of the second campaign are similar to the first one, confirming those observations but they are not discussed in detail.

1st measurement campaign of task 3

Two different catalyst setups were utilized. Both utilized urea for NO_x reduction, but the oxidation targets were different. The first setup consisted of a combination of a separate oxidation catalyst and an SCR catalyst. The oxidation catalyst, placed upstream of the SCR (and upstream of the urea injection), was targeted for methane oxidation (methane oxidation catalyst, MOC). The MOC utilized platinum-palladium (1:4) as active metals on a tailored coating developed for lean NG applications and supported on a metallic substrate. The volume of MOC was 1.69 dm^3. The SCR catalyst was a stabilized TiO_2-WO_3 based vanadium catalyst supported on a metallic substrate with a volume of 5.5 dm^3. The other setup consisted of only one catalyst reactor (OXICAT-x, placed similarly to the SCR in the first catalyst setup, see Figure 14), which targeted to the oxidation of carbon monoxide and formaldehyde and at the same time could utilize ammonia for NOx reduction. This OXICAT-x utilized a noble metal-Vanadium-Tungsten-Titania catalyst. The volume of OXICAT-x was 5 dm^3.

In order to study the performance of catalysts, the exhaust gas temperature and the space velocity are essential parameters. Studies were conducted in exhaust gas temperature range of 350 to 500°C and with two exhaust gas flows (80kg/h and 40kg/h). High temperature is needed for methane oxidation, and would also mean that the catalyst placement in any real application would be first in line downstream of the engine, even pre-turbocharger. The utilized flows result to space velocities (1/h) of 8600 and 4300 for the MOC+SCR system and 12400 and 6200 for the OXICAT-x system. A minimum of three test repetitions were made for each test condition in order to obtain reliable results.

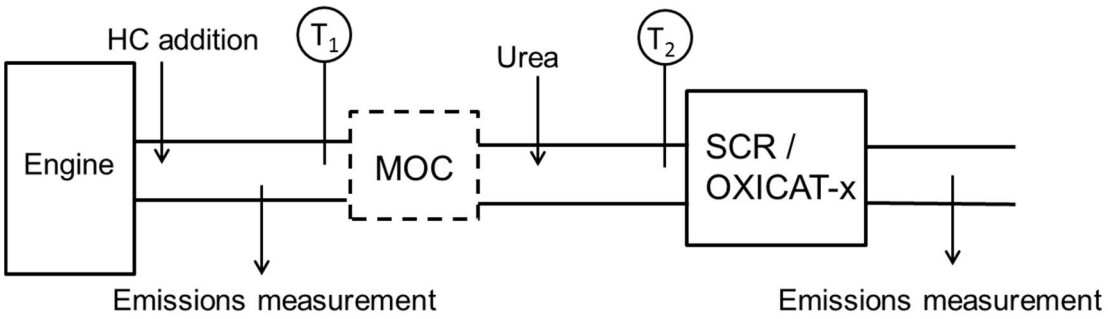

Figure 14 Test setup.

The sampling and measurement setup was similar to the one in task 2.

Before conducting any actual tests, the catalysts were preconditioned by aging for 48 hours in mode 1 (with an exhaust gas temperature of 400 °C and exhaust flow of 80kg/h, Table 2), without any urea feed. After the preconditioning, preliminary tests were performed for both catalyst setups in order to determine the urea feed to be utilized in subsequent tests. Aqueous 32.5% urea solution was used as reagent. Figure 15 shows an example of these preliminary tests resulting to the NO_x reduction and NH_3 slip as a function of urea feed (NH_3/NO) in mode 1 for the SCR.

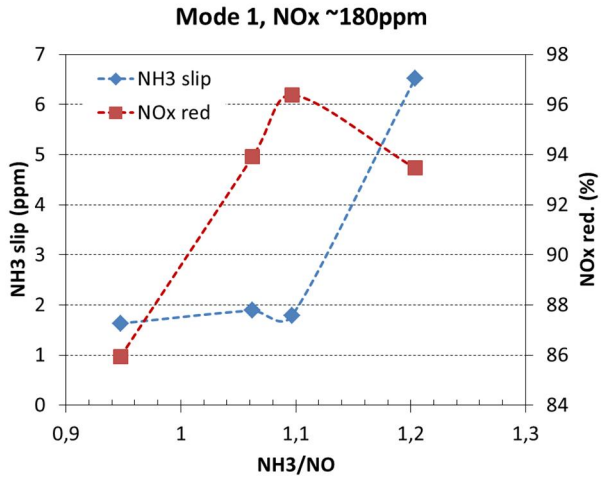

Figure 15 NO_x reduction and NH_3 slip measured as function of NH_3/NO (note. Four measurement points and the lines are to guide eye only).

The urea feed was selected to have a condition in which no (or only minor, i.e. below 5 ppm) ammonia slip was formed in the catalyst and the NOx reduction was still clearly above 90%. The used NH_3/NO_x ratios were 1.12 and 1.17 in mode 1 and mode 2 (see Table 2), respectively. This preliminary test was made only at an exhaust temperature of 400°C, and in further tests in different exhaust temperatures the urea feed was kept the same. It should be noted that this most probably did not result in the SCR's best possible performance in all the selected temperature modes.

Table 2 Driving modes (note. the modes are not the same as in task 1 since the engine control was modified after task 1).

	Mode 1	**Mode 2**
Torque	70 Nm	35 Nm
Speed	2700 rpm	3100 rpm
Power	20 kW	12 kW
O_2	6.0 %	6.3 %
NO_x	190 ppm	50 ppm
CO	400 ppm	430 ppm
Hydrocarbon additions	No	Yes

The emission measurement setup was similar to the setup utilized in task 2 (see Figure 5).

Many results presented here are also published in Lehtoranta et al. 2016.

Urea decomposition

Good urea decomposition is a basis for efficient SCR operation and for avoiding misuse of the catalyst itself for water evaporation and urea decomposition. Furthermore, the urea decomposition as well as the droplet size and mixing of urea with exhaust gas should be similar to that occurring in a real application case, in order to make the present studies in an engine laboratory comparable with real application cases. For example, in the present study the distance from the urea injection to the catalyst entrance and the nozzle utilized for urea injection were selected on the basis of the authors' knowledge of real application setups.

In order to determine how the injected urea is decomposed to ammonia, measurements were made upstream of the SCR but downstream of the urea injection. These measurements were made using the FTIR. Urea decomposition occurs in phases (e.g. Koebel et al 2003, Yim et al 2004). First, the water from the urea solution droplets is evaporated. Then the urea is thermally decomposed into ammonia (NH_3) and isocyanic acid (HNCO). Hence, 1 mol of urea produces 1 mol of ammonia and 1 mol of isocyanic acid. The isocyanic acid is quite stable in the gas phase, but readily hydrolyzes on the surface of a metal oxide catalyst, producing ammonia and carbon dioxide. The measurements showed that at a temperature of 350 °C approximately 50% of the urea was decomposed to ammonia and isocyanic acid, whereas at higher temperatures the decomposition rate was clearly higher: at 400-450 °C almost 80% of the urea was decomposed (Figure 2). This is clearly better than the results reported earlier for decomposition of urea for automotive SCR systems by Koebel et al. (2003), who found that only about 50% of urea decomposed at 400 °C when the residence time from urea injection to catalyst entrance was 0.09s. In the present study the residence time was longer: at 400 °C the residence time was 0.13s. The time available from the injection to the catalyst entrance is one of the key issues when discussing urea decomposition (Koebel et al. 2003) and also one possible reason for the differences in urea decomposition between the present study and the study by Koebel et al. (2003). Other possible reasons could be a smaller droplet size or a better mixing of urea with the exhaust gas.

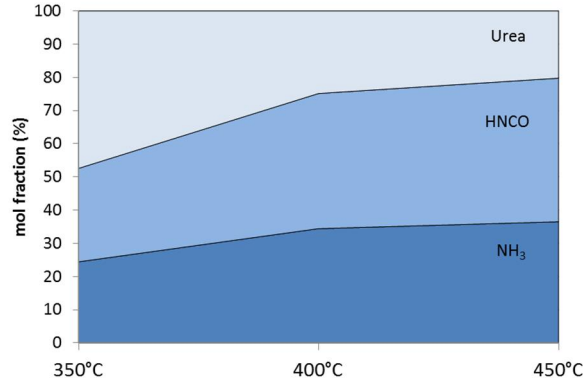

Figure 16 Urea decomposition (Lehtoranta et al. 2016)

Gasous emissions

The NO_x reduction, calculated from the NO_x measurements upstream and downstream of the catalyst, is presented as a function of temperature (measured upstream of the SCR or 'oxicat-x' i.e. T2 in setup figure) in figure 17 at constant urea feed. The conventional SCR (placed downstream of the MOC) seem to operate similarly at both driving modes and the NO_x efficiency (%) seems to depend on the temperature only little between 350-450 °C.

The NO_x efficiency of oxicat-x, however, was found to depend greatly on the temperature since a clearly smaller efficiency was measured at the highest test temperature of 450°C, especially in the case of mode 2. The lower NO_x reduction by 'oxicat-x' is probably due to the competing reactions that actually oxidize the injected ammonia to NO instead of the reaction between ammonia and NO resulting to N_2. One should also note that the urea injection was not optimized for the different temperatures but was constant.

Since the two catalyst systems are different e.g. in compositions, volumes, catalyst loadings, one could also expect to have differences in NO_x reductions. However, at exhaust temperature of 400°C both catalyst systems seem to operate rather similarly (with the same urea feeds) reaching NO_x reduction near 95% ('oxicat-x' reaches even higher at mode 1). As anticipated, differences are observed at the other test temperatures. In standard SCR catalyst the optimal operation window depends greatly e.g. on the catalyst (vanadium) loading (e.g. Forzatti et al. 1996, Lietti et al. 2000, Lehtoranta et al. 2015). High vanadium loading increases NO_x reduction at low temperatures but the higher the vanadium loading is the more the SCR also oxidizes NH_3 at high temperatures. E.g. a recent study of the differently loaded vanadium SCR's performance (in heavy fuel oil application) resulted to a rather similar NO_x efficiency with all tested catalyst loadings at the 350-450°C but at lower temperatures the highest loaded catalyst resulted to significantly better NO_x efficiency compared to lower loaded catalysts (Lehtoranta et al. 2015).

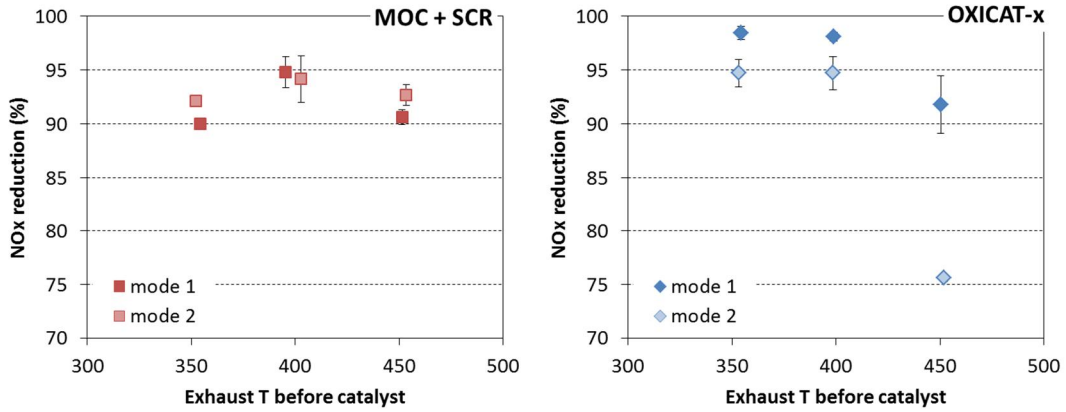

Figure 17NO_x reduction for MOC+SCR and Oxicat-x (Lehtoranta et al. 2016)

The measured methane concentrations (in mode 1) are shown in Figure 18 as a function of the exhaust temperature measured upstream of the oxidation catalyst (T1 for MOC and T2 for OXICAT-x – see setup figure). For both catalyst setups three different exhaust temperature modes were studied, as well as a lower exhaust flow mode in one selected temperature case. The OXICAT-x was not designed for methane oxidation and therefore it was not expected to have any effect on the methane levels. This was found to be true on the basis of the measurement, since the OXICAT-x had practically no effect on methane in either of the studied exhaust temperatures or flows. The MOC+SCR, with the methane oxidation catalyst, had a minor decreasing effect on the methane at ~400°C, but at ~500°C approximately 50% methane decrease was observed. Furthermore, the lower exhaust flow studied at 450°C increased the methane conversion from 38% (measured with 80kg/h exhaust flow) to 65% (with 40kg/h).

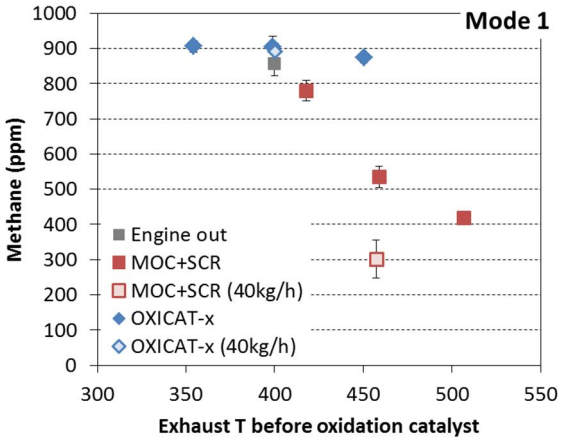

Figure 18 Methane level as a function of exhaust temperature (Lehtoranta et al. 2016)

In addition to methane, other hydrocarbon species i.e. ethane, propane and ethylene were also studied. The ethane and propane concentrations as a function of exhaust temperature in mode 2 (see table 2) are presented in Figure 19. The OXICAT-x started to oxidize these hydrocarbon species at the exhaust T of 450°C, whereas at lower temperatures practically no effect was found. At the same temperature (450°C) the MOC, as expected, oxidized ethane and propane more effectively than OXICAT-x and the oxidation also increased with the temperature increase (500°C). At 450°C the ethane conversions were 37% with OXICAT-x and 65% with MOC and the propane conversions were 75% with OXICAT-x and 88% with MOC. Thus, the alkane reactivity proceeds in the order $C_3H_8 > C_2H_6 > CH_4$, which is as was expected and similar to the observations of e.g. Lambert et al. (1997) and Ottinger et al. (2015). The ethylene was the easiest to oxidize, and practically no ethylene was measured downstream of either of the catalyst setups.

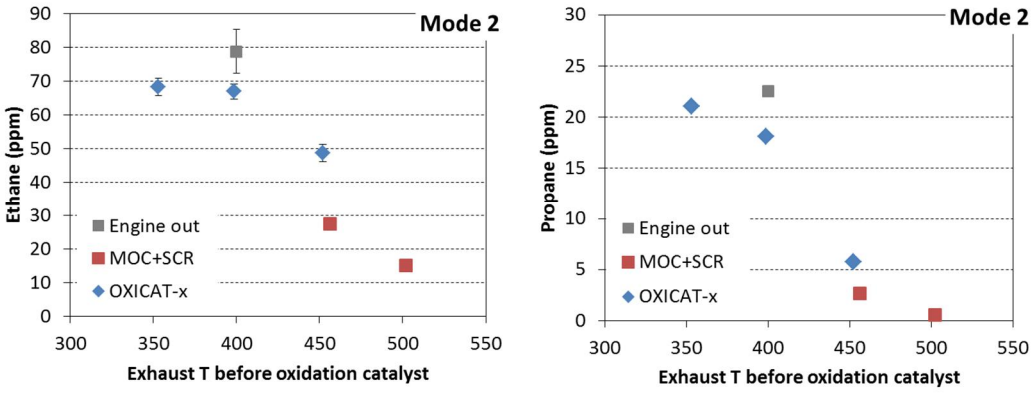

Figure 19 Ethane and propane levels as a function of exhaust temperature (Lehtoranta et al. 2016)

Particle emissions

One standard (ISO 8178) method was utilized to study the particle mass emission. Since the PM method measures the total mass, larger particles can contribute to the result much more than smaller ones (nanoparticles).

Engine out PM results had a rather high variation of 17% (standard deviation of 4-5 samples) (Figure 20). The effect of the catalysts was however obvious, and both catalyst systems clearly decreased the total PM in all test conditions. The PM reduction was of the order of 45-73%. Since catalysts commonly have a decreasing effect only on the volatile (organic) fraction of the PM mass, this alone indicates that a large part of the engine out PM is some volatile material present in gaseous phase at the catalyst temperatures.

However, the PM results measured downstream of the catalysts appeared to correlate with the exhaust temperature, as higher PM levels were measured at higher exhaust temperatures (with 'the mode 1 and 500°C' case forming an exception to this pattern, see Figure 20). Sulphate formation contributing to PM increase is seen over many catalysts (ammonium sulphates in the case of SCR), and could be one explanation for the PM increase with temperature increase, although in the present study the total amount of sulphur available from the fuel and oil was very low.

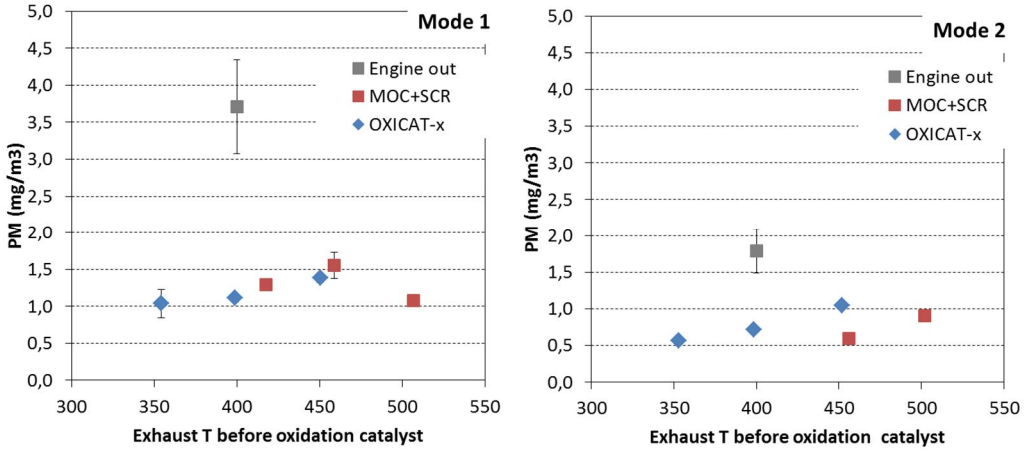

Figure 20 PM (Lehtoranta et al. 2016)

Engine out returned qualitatively similar results for particle number to those obtained previously (Task 2, Alanen et al. 2015); particle number size distribution was dominated by nanoparticles smaller than 10 nm, and especially the smallest particles were observed to be non-volatile. The thermodenuder treatment was observed to decrease the concentration of larger particles (diameter > 5 nm), shifting the mean particle size to a smaller level, which indicates that the particles also contained some semi-volatile compounds.

When the exhaust was sampled for particle measurements downstream from the catalyst, the exhaust temperature was observed to significantly affect the particle number (see Figure 22) and number size distribution (Figure 21). First, at the lowest temperature the measured particle numbers were lower than those in the sample from upstream of the catalyst. The catalyst was observed to affect all particle sizes. However, the particle number was also dominated by nanoparticles downstream from the catalyst. When the exhaust temperature was increased, both the mean particle size and the particle number concentration (measured downstream from the catalyst) increased. At the highest temperature point (500 °C) the particle size distribution was dominated by particles larger than 10 nm and the total particle number (measured by PSM, particles larger than ~1 nm) was up to 20 times higher than the concentration at the lowest temperature point, and more than five times higher than the particle number in the sample taken upstream from the catalyst.

The increase in particle number as a function of exhaust temperature was caused by volatile particles; the thermodenuder treatment for the exhaust sample totally removed the particle mode at 10 nm (Figure 21). Based on previous studies, conducted mostly on diesel engines, the volatile exhaust particles have been observed to be formed during cooling and dilution of exhaust (Lähde et al. 2009; Rönkkö et al. 2013), especially when the engine is equipped with

an oxidative exhaust after-treatment device (Maricq et al 2002; Vaaraslahti et al. 2004; Kittelson et al 2008, Lähde et al. 2009). One possible precursor for nanoparticle formation is sulphuric acid, which is present in gaseous phase at typical exhaust temperatures and tends to nucleate in exhaust sampling systems (see e.g. Olin et al 2015, Pirjola et al. 2015), forming new particles. However, organic acids have also been proposed to participate in this process (Arnold et al. 2012). The observations of this study are qualitatively similar to those of studies in which the role of sulphuric acid in particle formation has been measured; nanoparticles are volatile, they exist in the sample taken after the catalyst and an increase of exhaust temperature increases particle concentration and size. The particle composition measurements (see the text below) support the notion that sulphur compounds may explain these observations.

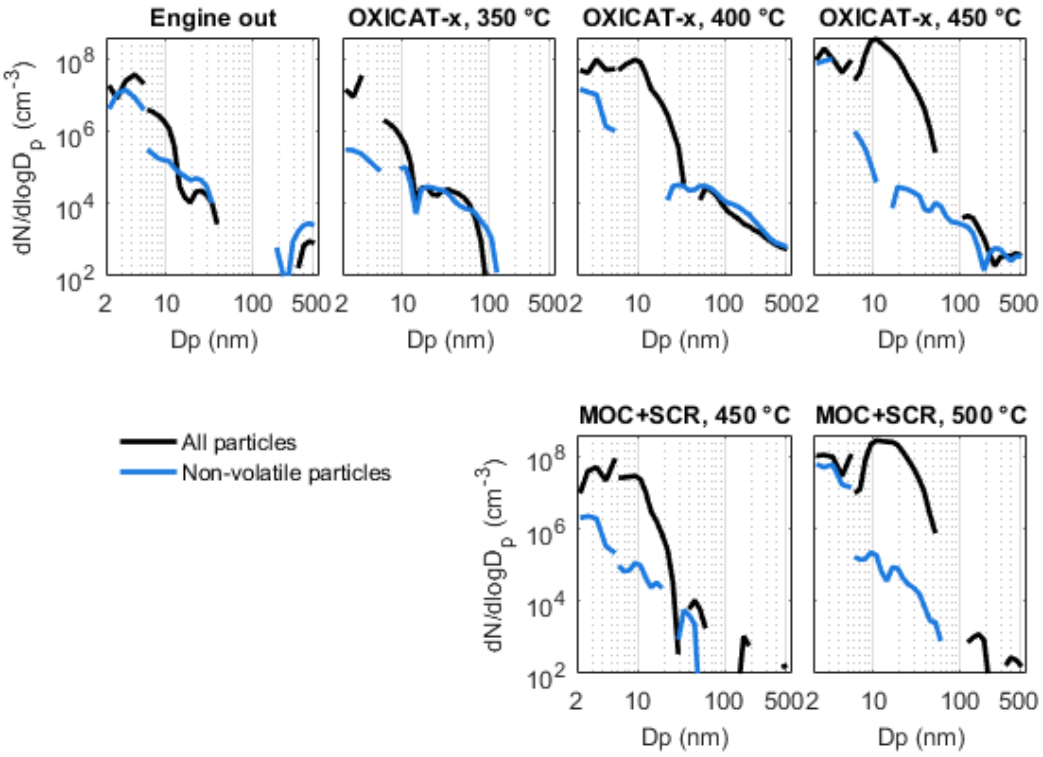

Figure 21Particle number size distributions upstream from the catalyst (engine out) and after the catalyst at different exhaust temperatures. Both the distributions measured without the thermodenuder (all particles) and with the thermodenuder (non-volatile particles) are shown. Size distributions were measured by the combination of PSM and CPC and by the EEPS in mode 2.(Lehtoranta et al. 2016)

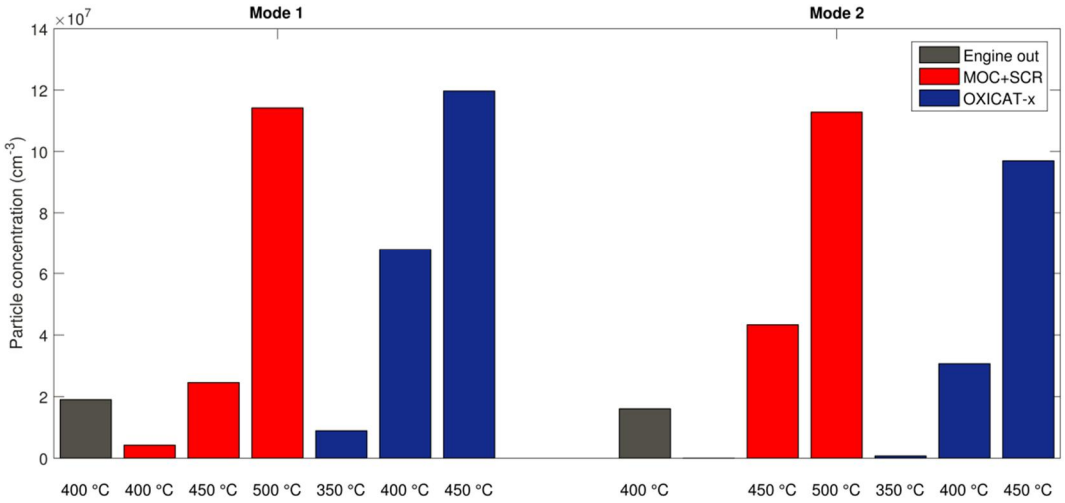

Figure 22 Total particle number concentration of natural gas engine exhaust when the exhaust was sampled upstream from the catalyst (engine out) and after the catalyst. Particle concentrations were measured by the combination of PSM and CPC. (Lehtoranta et al. 2016)

Based on the SP-AMS results the concentration of sulphate increased with higher catalyst temperature (Figure 23). Sulphate was clearly higher at 450 °C for OXICAT-x and MOC+SCR in mode 1 and at 500 °C for MOC+SCR in mode 2. At an exhaust temperature ≤450 °C the sulphate concentration measured downstream from the catalyst was lower than that measured upstream of the catalyst, but at 500 °C (MOC+SCR) it was more than double that measured upstream of the catalyst. Ammonium had similar temperature dependence to that of sulphate. Sulphate appeared to be mostly neutralized with ammonia, as their ratio was close to that calculated for ammonium sulphate. Only at the highest catalyst temperatures (and sulphate concentrations) was there excess sulphate, suggesting that a part of the sulphate was in the form of sulphuric acid in particles. The amount of sulphuric acid ranged from 12–27% of the measured sulphate, corresponding to sulphuric acid concentrations of 2–22 µg m-3. However, it should be noted here that the SP-AMS can detect particles only above ~50 nm in size, meaning that only the tail of the particle mode shown in the particle number size distributions of Figure 21 was measured by the SP-AMS. In addition to sulphate and ammonium, nitrate concentration also increased with the catalyst temperature increase, although the catalysts decreased the concentration of nitrate by as much as 87% on average.

In addition to sulphate, ammonium and nitrate, particles contained organic matter, chloride and black carbon (Figure 24). Excluding the measurement points with high sulphate concentrations, most of the particle mass consisted of organic matter. The concentration of organic matter had no clear dependence on the catalyst temperature, but the catalysts reduced organic matter by on average 86% (OXICAT-x) and 55% (MOC-SCR). This is in good correlation with the PM results, showing that the total mass was clearly reduced by the catalysts. Chloride also showed no trend with the catalyst temperature, and the concentration of chloride was only slightly lower with the catalysts. Black carbon was observed to exist in the exhaust only in engine out measurements.

Organic matter in the gas engine emission particles was mostly composed of hydrocarbon fragments (Figure 25). The largest hydrocarbon fragments according to the mass spectra (MS) of organic matter were $C_3H_5^+$ (at m/z 41), $C_3H_7^+$ (at m/z 43), $C_4H_7^+$ (at m/z 55) and $C_4H_9^+$ (at m/z 57), typical for e.g. vehicle emissions (e.g. Canagaratna et al., 2004, Chirico et al., 2011). Similar to sulphate, ammonium and nitrate, the sum of hydrocarbon fragments increased with the catalyst temperature (Figure 23), but the catalyst decreased the concentration of hydrocarbons much more than those of inorganics. As well as the

hydrocarbon fragments, there were some oxidized organic fragments, e.g. $C_2H_3O^+$ (at m/z 43) in the MS. In general, no change in the oxidation state of organics was observed as a result of the catalysts.

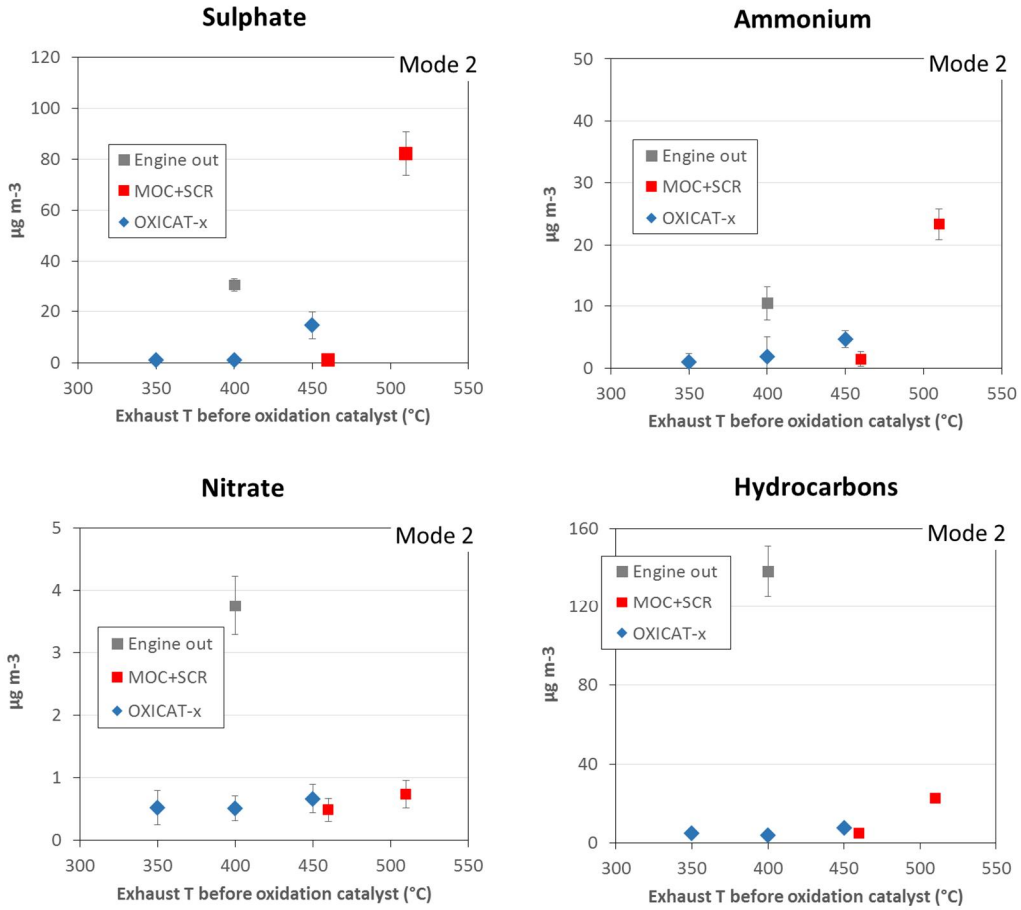

Figure 23 Sulphate, ammonium, nitrate and hydrocarbon concentrations as a function of exhaust temperature (measured upstream of the oxidation catalysts) for Mode 2 (Lehtoranta et al. 2016).

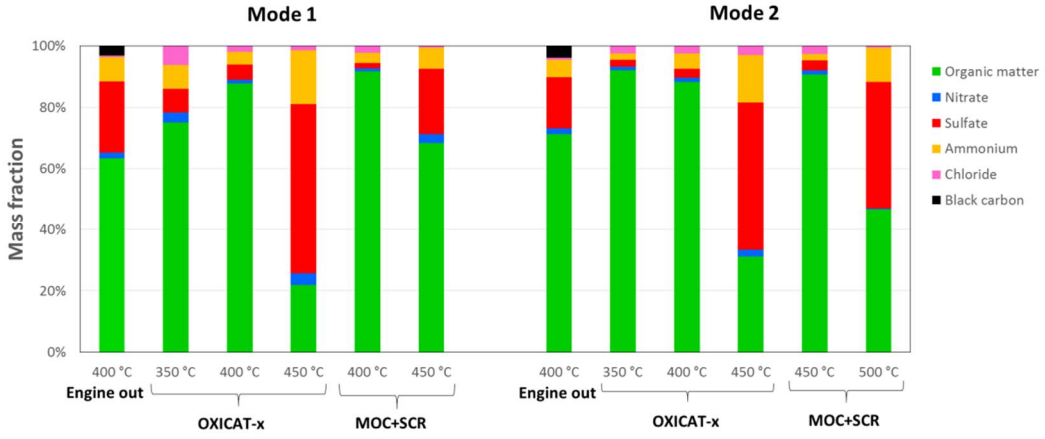

Figure 24 Chemical compositions of particles at various measurement points (Lehtoranta et al. 2016)

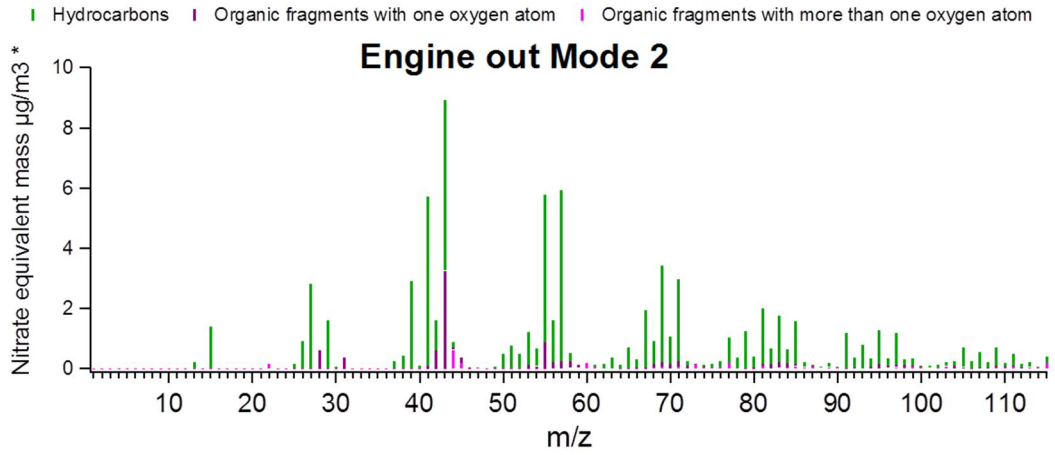

Figure 25 Mass spectra for particulate organic matter measured without the catalysts in mode 2 (Lehtoranta et al. 2016).

Secondary particle formation

A potential aerosol mass (PAM) chamber was used to simulate the aging process of the natural gas engine exhaust in the atmosphere. In the PAM, an oxidative environment was produced by two UV lamps emitting 185 nm and 254 nm radiation in a small (13 l) flow-through chamber. The PAM chamber was placed between the two dilution stages and the flow through it was a constant 5 l/min (residence time 156 s), measured by a bubble flow meter (Gilibrator, Sensidyne Inc.) and adjusted by a pressure regulator of the compressed air flow to ejector diluter.

The PAM chamber could be either bypassed or used in order to measure the properties of primary and secondary aerosols, respectively. The approximate atmospheric age, i.e. photochemical age simulated by the PAM chamber UV-lights, was modelled using the properties of the PAM chamber and the measured concentrations of gaseous components that cause external OH reactivity in the chamber. The PAM OH exposure is described here as photochemical age which is the equivalent time in the atmosphere in which the sample would reach the same OH exposure as in the PAM chamber. Thus,

$$\text{Photochemical age (days)} = \frac{\text{OH exposure}}{1.5{*}10^{6}\ \text{molec. cm}^{-3}} \frac{1}{3600\ \text{h}^{-1}\ \text{s}{*}\ 24\ \text{d}^{-1}\ \text{h}} \quad (2)$$

where $1.5 * 10^{6}$ molec. cm^{-3} is the average OH concentration in the atmosphere.

The secondary particle formation potential was measured using a high-resolution low-pressure impactor (HRLPI) in addition to EEPS and SP-AMS.

Reliable results for the secondary aerosol formation potential were measured at those engine mode – catalyst combinations that are presented in Figure 26. M denotes engine mode, C catalyst and the temperature tells temperature prior to the oxidation catalyst. The PAM chamber was used with a constant UV-light voltage that resulted in an equivalent atmospheric age of 4.6-10.7 days. The studied retrofitted natural gas engine was observed to have a low or moderate secondary particle formation potential, although the simulated atmospheric ages were relatively long. The secondary organic aerosol (SOA) formation potential was measured to be 8-18 mg kg_{fuel}^{-1}. The longest atmospheric ages produced both the highest secondary organic aerosol and the secondary particulate mass concentrations.

However, the mass of total aged particles, i.e. particle mass measured downstream the PAM chamber, was 6-170 times as high as the mass of the emitted primary exhaust particles. The total aged particles consisted mainly of nitrate, organic matter, sulfate and ammonium, the fractions depending on exhaust after-treatment and used engine parameters. Also the

volatility, composition and concentration of the total aged particles were found to depend on the engine operating mode, catalyst temperature and catalyst type. For example, a high catalyst temperature promoted the formation of sulphate particles, whereas a low catalyst temperature promoted nitrate formation. However, especially the concentration of nitrate needed a long time, more than half an hour, to stabilize, which complicated the conclusions but also indicates the sensitivity of nitrate measurements on experimental parameters such as emission source and system temperatures.

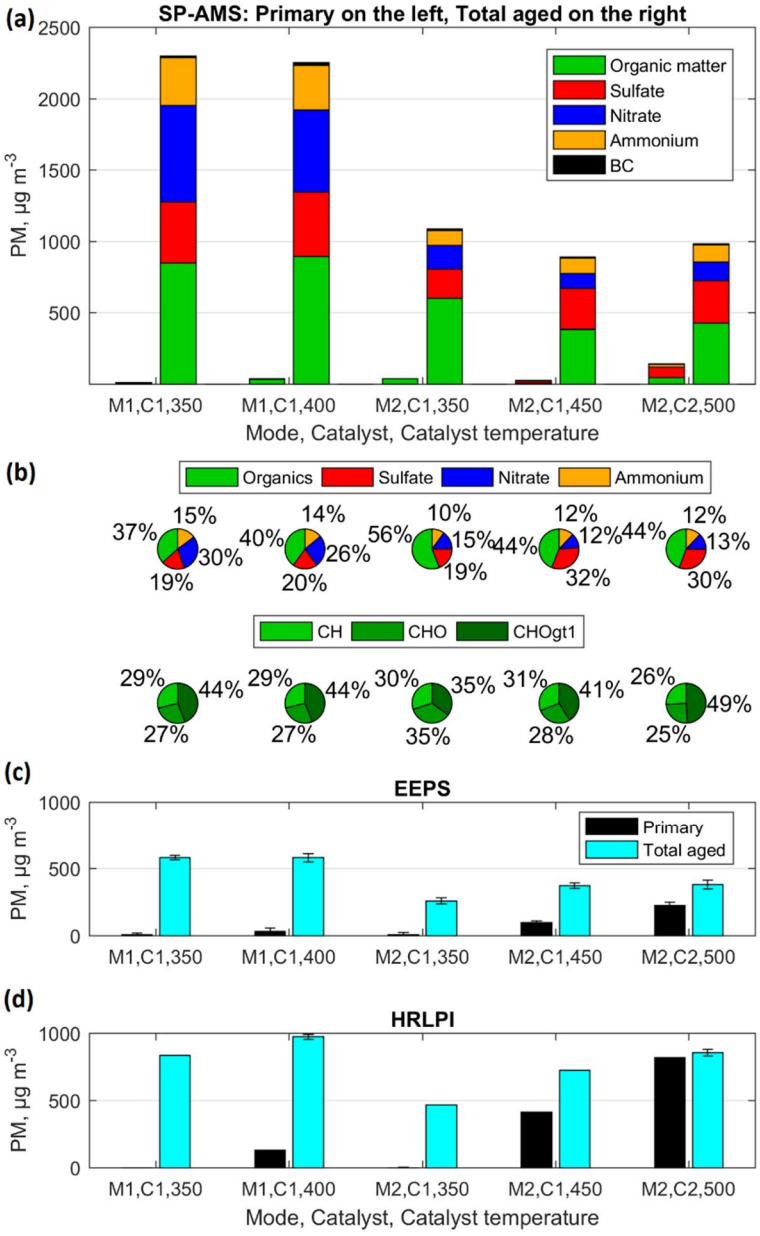

Figure 26 Exhaust primary and total aged particle mass concentrations measured by (a) SP-AMS, (c) EEPS and (d) HRLPI at different engine modes and catalyst temperatures. All values have bean corrected by dilution ratio used in the sampling system. Secondary particle mass can be calculated by subtracting primary from total aged emission. The composition of the total aged particulate matter and the organic particulate matter is presented as pie charts (b). The fraction of black carbon is less or equal to 1 % and therefore left out from the pie charts (Alanen et al. 2017).

Table 3 Secondary organic aerosol production factor, formed secondary particulate matter concentration from the NG engine, and the atmospheric age simulated by the PAM chamber

	M1, C1, 350 ◦C	M1, C1, 400 ◦C	M2, C1, 350 ◦C	M2, C1, 450 ◦C	M2, C2, 500 ◦C
SOA production factor (mg kg_{fuel}^{-1})	17	18	12	8	8
Total secondary concentration (µg m^{-3})	2299	2253	1089	890	986
Atmospheric age (days)	10	10.7	4.6	4.7	9.3

Sulphate was measured to have the highest evaporation temperature and nitrate the lowest (Figure 27). The evaporation temperature of ammonium depended on the fractions of nitrate and sulphate in the particles. The average volatility of the total aged particles was measured to be lower than that of primary particles, indicating better stability of the aged natural gas engine emitted aerosol in the atmosphere.

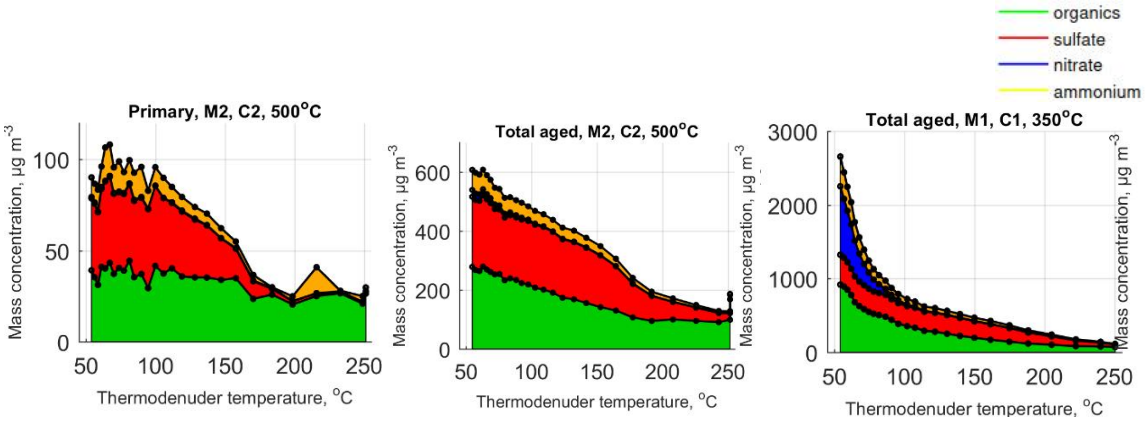

Figure 27 Concentration of different chemical compounds of particles remaining after the thermodenuder treatment conducted for the exhaust aerosol. The mass concentrations were measured using the SP-AMS at different thermodenuder temperatures and corrected by the dilution ratio used in the sampling system.

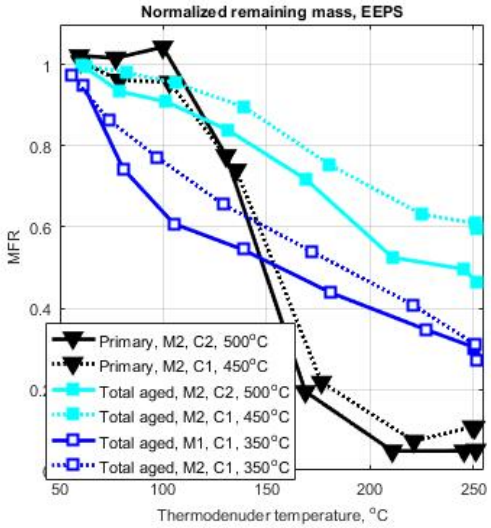

Figure 28 Results of particle volatility measurements. Particle mass fraction remaining (MFR) after the thermodenuder treatment for the exhaust aerosol sample of three different types of particle emission from the natural gas engine. MFR values were calculated from the size distributions measured by EEPS with unit mass assumption.

According to the results of this study, the shift from traditional liquid fuels to natural gas can have a reducing effect on total particle pollution in the atmosphere; in addition to the very low primary particle emissions, also the secondary organic aerosol formation potential of natural gas exhaust was lower or on the same level as the SOA formation potential measured on liquid fuels in previous studies.

Many results presented here are also published in Alanen et al 2017.

2nd measurement campaign of task 3

The engine setup for the second measurement campaign was similar to the first one of task 3. But the catalysts to be studied were different and also the lubricating oil was different.

The catalysts were: SCR+Oxi and Oxicat-y. The SCR was similar to the one utilized in first campaign but the oxidation catalyst was different since this time it targeted to non-methane components oxidation. The placement of the oxidation catalyst was right after the SCR. Oxicat-y was similar to earlier measurement's Oxicat-x, but now with significantly reduced volume. In the first campaign the Oxicat-x was found to be very effective in NOx, CO, aldehyde and ethylene reductions practically in all studied conditions.

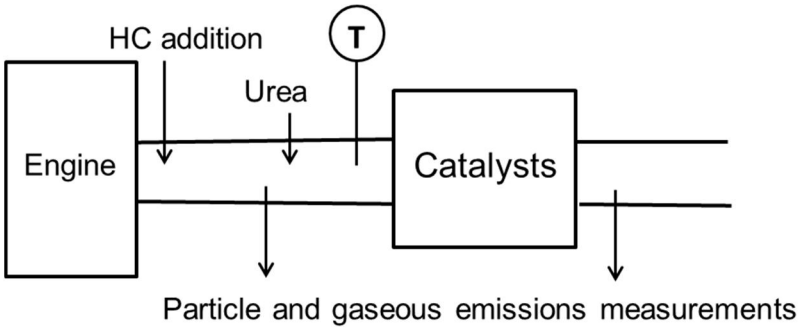

Figure 29 Setup.

The lubricating oil was similar to what is utilized in real scale gas engine power plants. This same oil is also utilized in the power plant engine of task 4 (see the next chapter). The lubricating oil sulphur content was >8000 mg/kg, density was 889.7 kg/m^3 and viscosity at 100 °C was 13.96 mm^2/s (see appendix).

The measurement setup was rather similar to the one in the first campaign of this task, but differed in sense of aldehyde and HC measurements. In this campaign the methane, ethane, propane and ethylene components were measured from dry exhaust gas sample with an online gas chromatograph (Agilent Micro GC) without dilution and the sample for aldehyde measurement was diluted utilizing the same system utilized for particulate mass measurement.

In this campaign in addition to the standard method ISO 8178, EPA 5 + EPA 202 were employed for particle mass measurement. These EPA 5 + EPA 202 methods are utilized for determination of particulate matter emissions from stationary sources in US.

In EPA Method 5 the particulate matter is withdrawn isokinetically from the source and collected on a glass fibre filter maintained at temperature 120 ±14 °C. The PM mass, which includes any material that condenses at or above the filtration temperature, is determined gravimetrically after the removal of uncombined water. This is called the Filterable Particulate Matter (FPM). EPA Method 202 defines the condensable particulate matter (CPM) which is

collected in dry impingers after filterable PM has been collected on a filter. Method includes procedures for measuring both organic and inorganic CPM. A consultant was employed for the EPA method measurements.

In the second campaign particle chemical composition was measured similar to the first campaign with the SP-AMS. The only difference between the first and second campaign was the dilution system for the SP-AMS; in the first campaign the SP-AMS measured after PTD and ejector diluter resulting the total dilution ratio of 24 whereas in the second campaign the SP-AMS measured only after PTD with the dilution ratio of ~10-11.

The sampling and dilution setup consisted of the same components as in the first campaign but the sample for SP-AMS and one CPC could be taken both upstream and downstream the ejector diluter. The particle number concentration and size distribution were measured by a CPC, ELPI+, EEPS, Nano-SMPS, Long-SMPS and PSM that have been introduced earlier in

Gaseous emissions

Since the engine modes are adjusted utilizing the NO_x sensors, the engine out NO_x levels, naturally, resulted to the same level than in the first campaign of this task. Also, the CO, HC and aldehyde (engine out) levels were similar to the ones of the first campaign of this task.

The results from the studies with a less effective catalyst (Oxicat-y) show how the exhaust flow influences the achieved emission levels. NO_x levels and CO levels are depicted in Figure 30 . The exhaust flows of 80 kg/h and 40 kg/h were studied. In practice, the decrease from the 80 kg/h to 40 kg/h represents a case where the catalyst volume is doubled. For example, in mode 1, the NO_x reduction with 80 kg/h is ~35% while the lower flow (40kg/h) results to a NO_x reduction of 45%. The NH_3/NO was kept constant and the increase in the efficiency is also seen as decreased ammonia slip formation downstream of the catalyst. Similarly for CO, an 89% conversion is achieved with the higher flow and decreasing this to half increses the conversion to 98%.

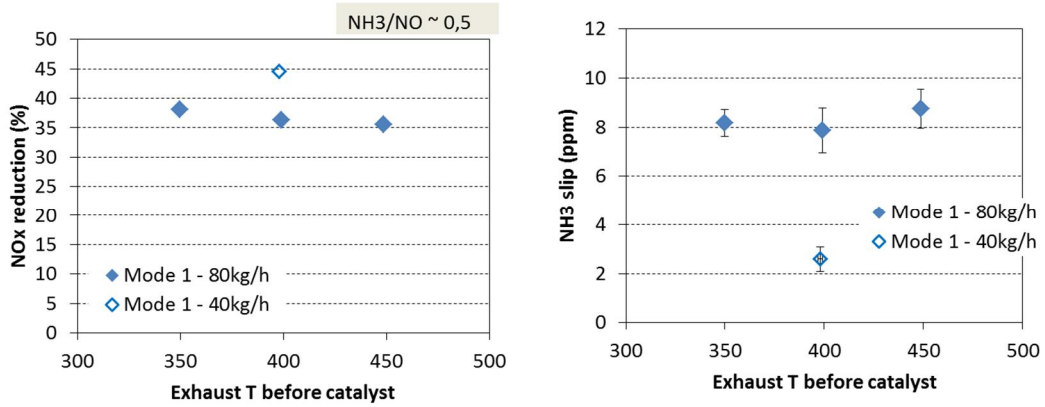

Figure 30 NO_x reduction and ammonia slip for Oxicat-y.

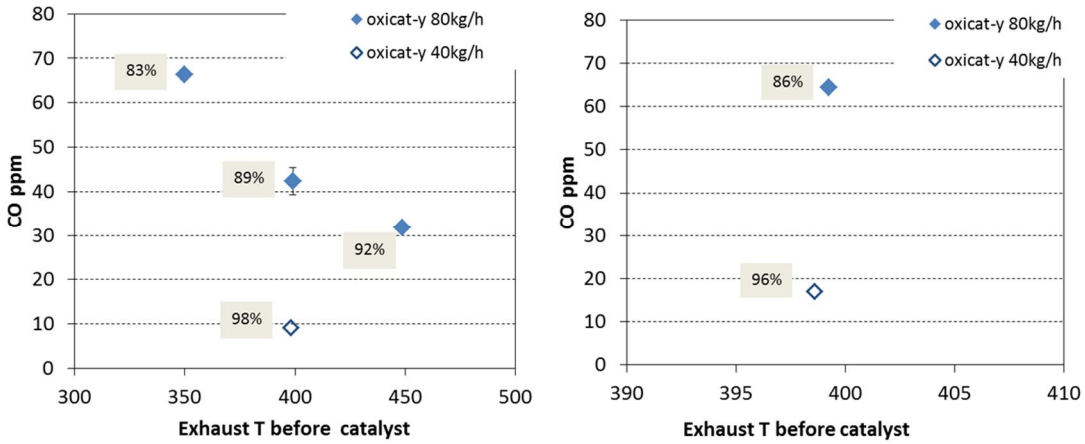

Figure 31 CO measured downstream of oxicat-y and the reductions achieved from the engine-out level (mode 1 at left hand side and mode 2 at right hand side).

Although, not shown here in detail, the SCR+Oxi combination was found to be very effective in NO_x reduction e.g. the efficiency at 400°C with 80kg/h (mode 1) was found to be ~96% while the lower flow (40kg/h) resulted to even higher level of ~98%. The CO oxidation efficiency was found to be above 98% at all tested operation conditions with the SCR+Oxi, so it was not possible to make any conclusions about the CO oxidation and the temperature and/or the flow dependency.

By lowering the exhaust flow, clearly better hydrocarbon oxidations (ethane, propane) were achieved with both catalyst systems. As expected, at the exhaust temperatures tested, the methane was not oxidized at all over either of the catalyst systems while the ethylene was totally oxidized in all measurement modes. An exmaple of the results at mode 2 with the Oxicat-y is presented in the table 4.

Table 4 HC reductions over the catalyst measured at two different exhaust flows at 400°C.

Reduction %		Methane	Ethane	Propane	Ethene
Mode 2	80kg/h	0	0,3	15,7	100
	40kg/h	0	12,1	25,7	100

Particle emissions

Engine out

The results of the total PM levels measured with both methods (ISO 8178 and EPA 5 + EPA 202) are presented in Figure 32. The results from these two methods differ from each other's, which could be expected, since all the condensable matter taken into account in the EPA 202 method might not be measured with ISO 8178 method.

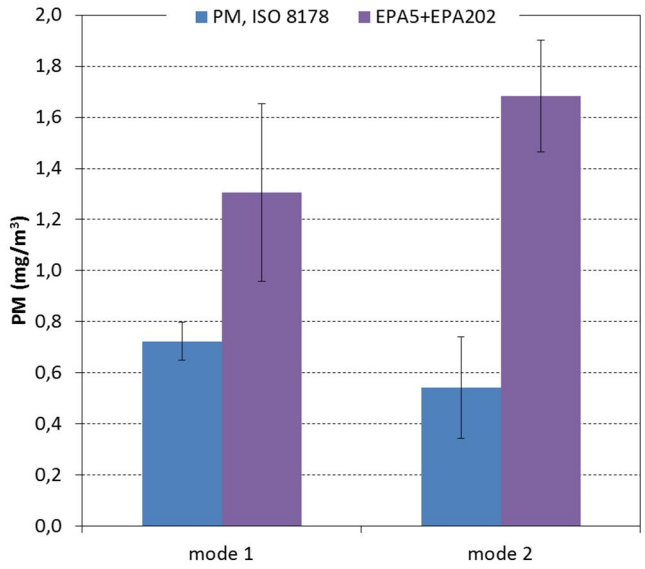

Figure 32 PM measured with ISO 8178 and EPA5+EPA 202 methods.

The engine out particle emissions were found to be at very low level and even at lower level than what was measured during the first campaign of this task. The engine out PM levels for both campaigns are presented at Fig. 33. Since the lube oil was the only parameter that was intentionally modified between these campaigns, this result indicates that the lube oil can have a significant effect on the PM formation in a natural gas engine exhaust.

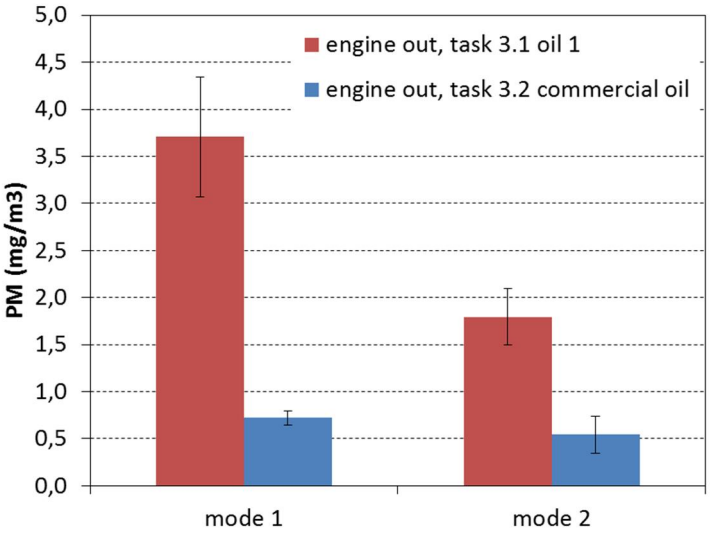

Figure 33 PM levels measured during the two campaigns.

Similar to the first campaign particles from the NG engine were dominated by organics the mass fraction of organics varying from 69 to 93%. Majority of organics was composed of hydrocarbon fragments; however, a much larger fraction of signal was caused by very small hydrocarbon fragments (e.g. CH_2^+, CH_3^+, CH_4^+) compared to that typically found for e.g. diesel fuel exhaust particles or in NG engine in previous campaign. The presence of small hydrocarbon fragments could be, at least partially, due to the dilution system as in the first campaign small mass fragments were not observed. Besides organics, particles contained e.g. sulphate, ammonium and black carbon.

Downstream of catalyst

Even though the engine out PM level was already at very low level, the PM measured downstream of the catalyst resulted to even lower levels than upstream. Similar to the first campaign the PM formation downstream of the catalysts seems to depend on the exhaust temperature i.e. higher temperature higher PM. The lower flow seems to result to lower PM levels but the standard deviation (of minimum of three repeated PM measurements) is rather large making it difficult to draw any final conclusions.

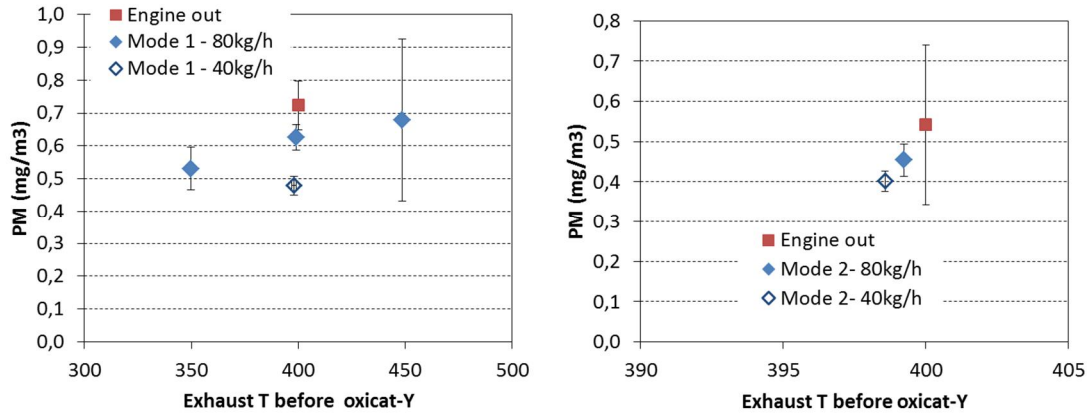

Figure 34 PM measured at upstream and downstream of catalyst (Oxicat-y) as a function of exhaust temperature at two different exhaust flow and two different driving modes.

Different from PM, mass concentration of submicron particles (< 1 µm in diameter) measured with the SP-AMS were larger downstream of the catalysts, but similar to the PM concentrations, submicron mass increased with the increasing exhaust temperature. In the first campaign the increase of submicron mass was caused by larger amount of sulphate in particles but in the second campaign sulphate mass did not increase with exhaust temperature. However, the increase of mass in the second campaign was due to a greater amount of organic matter in particles. So far, the reason for this is unclear and these results will be further analysed in the near future.

Regarding nanoparticles, at high temperatures (T ≥ 400 °C) both catalyst systems also increase the delayed primary nanoparticle emissions that form when exhaust is released into the atmosphere (Fig. 35). This phenomenon was found also in the first campaign. At the engine-out case and low catalyst temperatures the nanoparticle emissions did not differ from the zero level that was measured using only clean compressed air.

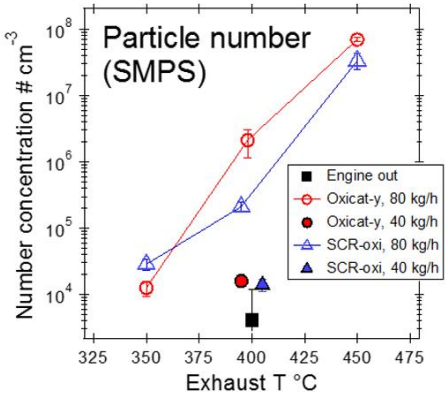

Figure 35 The dependence of particle number emission on exhaust temperature with and without exhaust after-treatment.

In the second measurement campaign the SP-AMS was also used to investigate metals in particles. V, K, Na, Cu, Fe, Zn, Cr and Ni were detected in NG emission particles. V, K and Na had clearly larger concentrations with Oxicat-y than with SCR+oxi or without the catalysts (Fig. 36). Additionally, the concentrations of those metals decreased with increased exhaust temperature with Oxicat-y. The concentrations of V, K and Na were elevated with Oxicat-y also when the exhaust flow was decreased (40 kg/h). Higher concentrations of metals observed with the SP-AMS for Oxicat-y than for SCR+oxi does not necessarily mean that the concentrations are larger in exhaust particles. It is possible that these metals were detected more efficiently with Oxicat-y due to the presence of black carbon in particles as the detection of metals with the SP-AMS is based on the absorbing material in particles (e.g. Onasch et al., 2012; Carbone et al., 2015). However, some metals can also absorb laser light themselves or can even be detected with the AMS without the laser. For example V was used as a constituent in both the catalysts but in particles after the catalyst the concentration was ~10 times larger for Oxicat-y than for SCR+oxi. For rBC concentrations the difference between Oxicat-y and SCR+oxi was smaller than for V but especially at 350 and 400 °C rBC was clearly larger for Oxicat-y.

Similar to V, K and Na, the concentrations of Cu, Fe and Zn were larger with Oxycat-y than with SCR+oxi, or engine out, but the difference between the measurement points was smaller. The concentrations of Cu, Fe and Zn increased with increasing exhaust temperature with Oxicat-y. With SCR+oxi the temperature dependence of Cu and Zn was less visible but Fe clearly decreased with increasing exhaust temperature. Cr and Ni did not follow the pattern of any other metals. Although they could be detected in the mass spectra, they did not have observable temperature patterns. However, Ni concentration was slightly elevated with the catalysts compared to that without them.

Besides as pure metal, V was also detected as it oxides. In catalysts vanadium is composed primary of vanadium pentoxide (V_2O_5). V_2O_5 was not detected in particles but with Oxicat-y there was signal for VO^+ and VO_2^+. All vanadium species decreased when exhaust temperature increased, however, for vanadium oxides the reduction in signal was slightly faster with temperature than for elemental vanadium. For iron, in addition to Fe^+ there was signal for FeO^+. At the exhaust temperatures of 350 and 400 °C the ratio of Fe+ to FeO+ was similar whereas at 450 °C FeO+ was not observed.

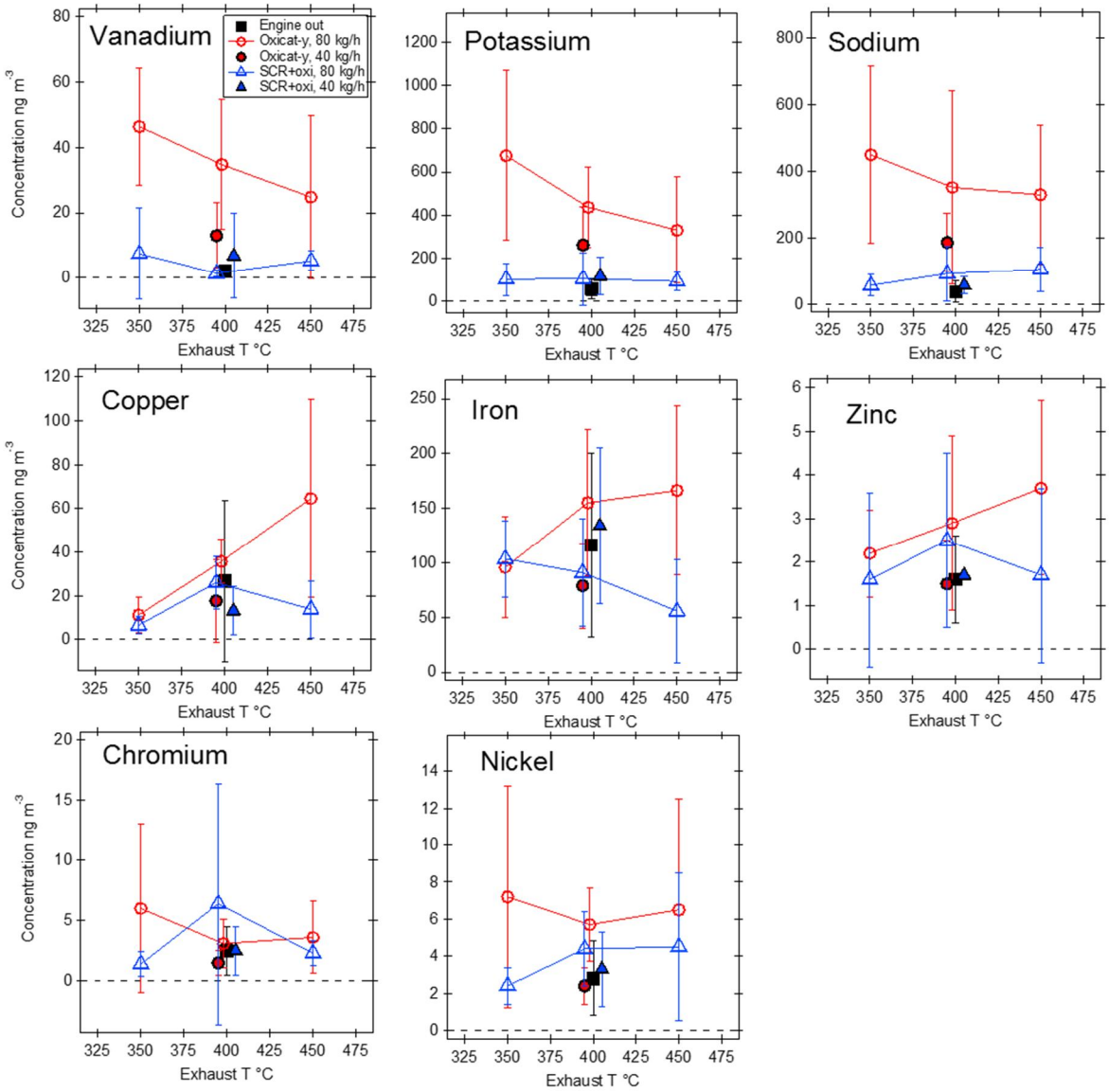

Figure 36 The effect of exhaust temperature and exhaust flow for the concentrations of selected trace elements in Mode 1.

Main findings of task 3

The SCR was found to be effective in reducing the NO_x. In present study, the SCR was utilized in three different ways, as a separate catalyst reactor downstream of a methane oxidation catalyst (MOC+SCR), upstream of an oxidation catalyst (SCR+Oxi) and as integrated into an oxidation catalyst (Oxicat-x and Oxicat-y). For the integrated system, and for the SCR+Oxi, the NO_x efficiency decreased at high temperatures. One explanation for this is that the oxidation reactions and NO_x reduction reactions are competing with each other resulting to lower NO_x efficiencies in high temperatures. This might form limitations for utilization; however, it greatly depends on the needed NO_x reduction as well as the possibilities to further optimize the behaviour in different temperature windows.

The results showed that the oxidation catalyst developed for methane removal can reach methane oxidation levels better than 50% in real natural gas engine exhaust gas application if the temperature is high and the catalyst sizing is correct. However, further studies are needed to solve the long term performance and the deactivation by sulphur.

Both the number concentration of the engine out nanoparticles and the PM mass at the second campaign of task 3 were significantly lower than at all the previous measurements at the same engine and fuel. The difference between the particulate matter emissions at the campaigns could be explained by lubricating oil: with the commercial lubricating oil the particle emission were lower than with the oil 1 or the oil 2.

Catalysts and exhaust temperature were found to have a clear effect on particle emissions. At both measurement campaigns catalysts were found to decrease the emissions of particulate matter total mass. However, according to the gained measurement results, nanoparticle number concentrations were increased by a catalyst combined with high exhaust temperatures. At the first campaign, the behaviour was connected to oxidation of sulphur compounds and generation of sulphuric acid and sulphates. At the second campaign, by contrast, the increase in particle emission at higher catalyst temperatures was due to an increase in organics.

Publications related to task 3:

Lehtoranta K., Murtonen T., Vesala H., Koponen P., Alanen J., Simonen P., Rönkkö T., Timonen H., Saarikoski S., Maunula T., Kallinen K., Korhonen S. Natural gas engine emission reduction by catalysts. Emiss. Control Sci. Technol. 2016, 1-11.

Lehtoranta K., Alanen J., Rönkkö T., Simonen P., Murtonen T., Vesala H., Saarikoski S., Timonen H., Maunula T., Kallinen K., Korhonen S. Particle emissions from a natural gas engine with and without a catalyst, ETH Nanoparticles 2016

Alanen, J., Simonen, P., Saarikoski, S., Timonen, H., Saukko, E., Hillamo, R., Lehtoranta, K., Keskinen, J., Rönkkö, T. Primary and secondary particle formation and volatility of natural gas engine exhaust. Submitted to Aerosol Chemistry and Physics in January 2017

Saarikoski S., Alanen J., Timonen H., Simonen P., Murtonen T., Vesala H., Rönkkö T., Aurela M., Maunula T., Kallinen K., Korhonen S. and Lehtoranta K. Characterization of natural gas engine emission by aerosol mass spectrometer. To be submitted 2017

Lehtoranta K., Murtonen T., Vesala H., Koponen P., Alanen J., Kuittinen N., Simonen P., Rönkkö T., Saarikoski S., Timonen H., Maunula T., Kallinen K., Korhonen S. Controlling emissions of natural gas engines. A&WMA's 110th Annual Conference, June 5-8, 2017

Task 4 - Real application study

Target: To conduct comprehensive emission studies and to study effects of new catalysts on emissions in power plant gas engine.

Experimental

The experimental study was done in real scale power plant engine at seven different load modes with emissions measurement upstream and downstream of the catalyst reactor. Emissions were studied from the exhaust of a spark-ignited lean-burn gas engine

The natural gas analysis results were: 91.2 % methane, 6.3 % ethane, 1.2 % propane, 0.42 % other hydrocarbons, 0.42 % nitrogen and 0.46 % carbon dioxide. The lubricating oil sulphur content was >8000 mg/kg, density was 889.7 kg/m^3 and viscosity at 100 °C was 13.96 mm^2/s (more detailed information can be found in the appendix).

The catalyst reactor contains catalysts with SCR and oxidative properties.

The emission formation was studied on different loads between 10 to 100%. Altogether seven load modes were run at 1-hour intervals. In addition three load modes were selected to run constantly several hours to study emissions requiring more time for sampling (e.g. PM collections). These three modes were one 100% load and two 10% loads. One of the 10% loads (10% B) was adjusted specially for this campaign to see the effect of the adjustment for emission formation. This was also studied in the 1-hour interval test run. The second 10% load (10% A) was the normal 10% load.

The emission measurement setup consisted of similar gaseous emissions analysers to task 2. The setup differed from the task 2 in case of aldehyde and HC measurement. In this case the HC components were measured from dry exhaust gas sample with an online gas chromatograph (Agilent Micro GC) without dilution and the sample for aldehyde measurement was diluted utilizing the same system utilized for particulate mass measurement. PM was measured following the standard ISO 8178-1:2006.

Particle number and size distribution measurements, performed by Nano-SMPS and ELPI, were done at all the tested engine loads. The sampling system was similar to the one that was used in tasks 2 and 3. The primary dilution ratio over the porous tube diluter was ca. 11 and the secondary dilution ratio over the ejector diluter was ca. 13. A thermodenuder was used to evaporate and absorb the volatile fraction of the particles. All emissions measurements were made upstream and downstream of the catalyst reactor (see Figure 37).

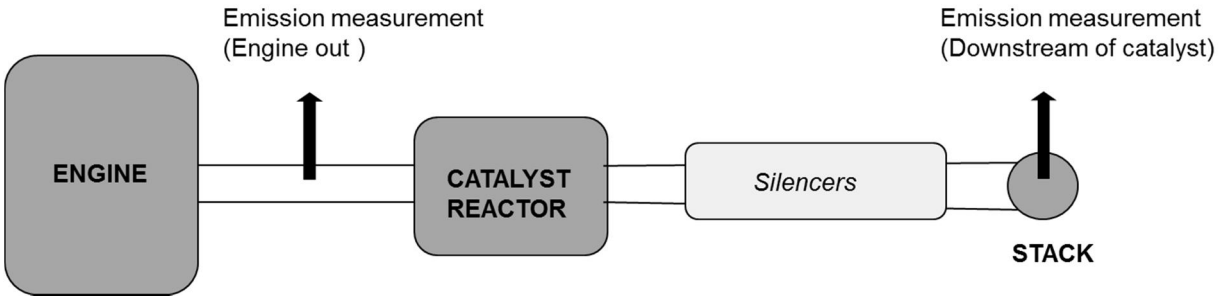

Figure 37 Setup.

Results – gaseous emissions

The engine out NO_x was found to decrease with decreasing engine load while the CO (and formaldehyde) increased with the decreasing load. The relative concentrations (scaled to the highest value) of NO_x, CO and formaldehyde measured upstream (engine out) are presented in Figure 38 as a function of engine load. Analysed hydrocarbons were methane, ethane, propane and ethylene. All these HC components behaved similarly when changing the engine load, the highest values were recorded at the 10% load while the lowest values at 100% load were only a few percent of the highest values.

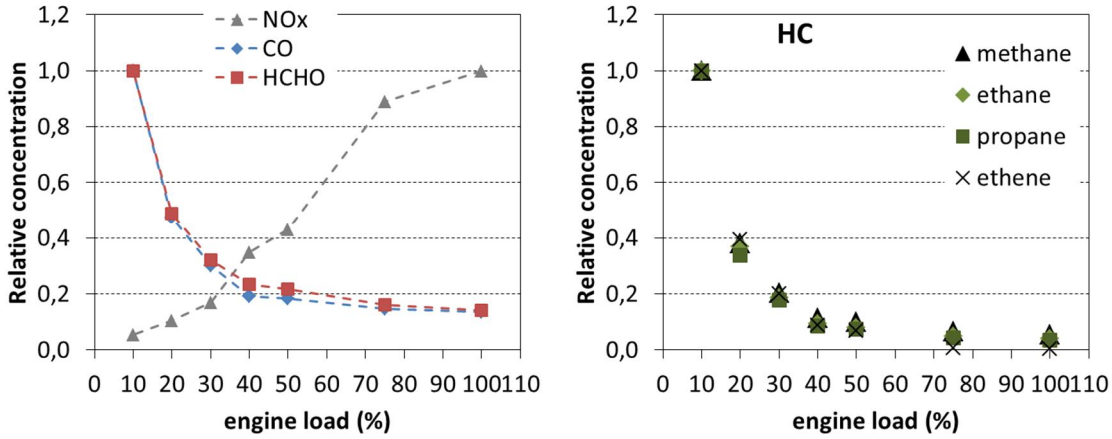

Figure 38 NO_x, CO, HCHO and HC concentrations as a function of engine load. Scale relative to highest value for NOx at engine load of 100% and for CO, HCHO and HC at engine load of 10%. The lines are to guide eye only.

The major HC component was methane. The portions of methane, ethane and propane of the total HC emissions were similar to the ones in the utilized fuel (i.e. natural gas).

The exhaust gas temperatures were between 366-414°C (measured upstream of the catalyst reactor, Table 6). The decrease of emissions over the catalyst is presented as conversions of different emission components in Figure 39. The results show that the catalyst was working very efficiently in targeting to low levels in NO_x by the SCR part and also low levels in CO by the oxidation catalyst part. The formaldehyde was effectively reduced by the catalyst reactor also. The CO and HCHO conversions over the catalyst were both above 95% at all engine load modes (Figure 39). The hydrocarbon levels increased with decreasing engine load. The SCR catalyst efficiency to reduce NO_x was found to decrease with the engine load decrease meaning that the lowest reductions were recorded at low loads where also the engine out NO_x levels were lowest.

Table 5 Exhaust gas temperatures, measured upstream of the catalyst reactor.

Load mode	Exhaust T (°C)
100	366
50	408
20	414
10	389

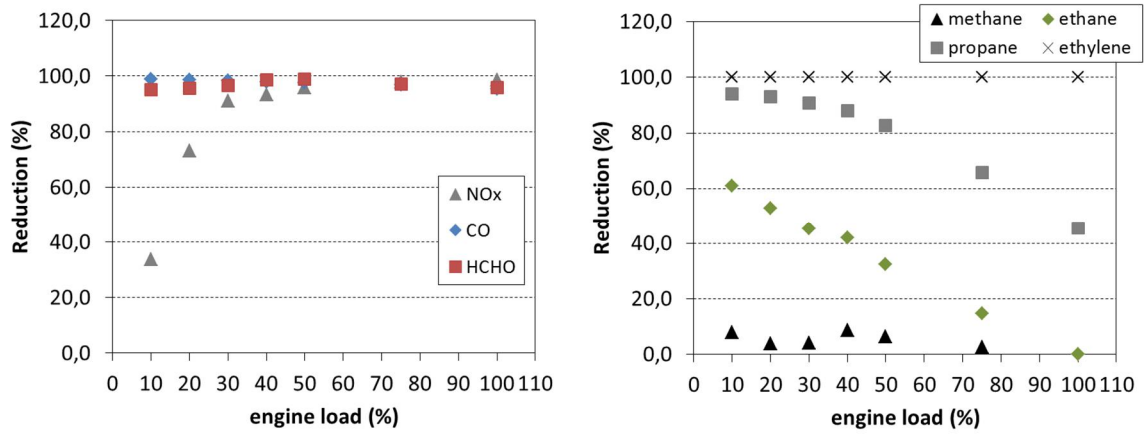

Figure 39 NO_x, CO, HCHO and HC conversions over the catalyst reactor as a function of engine load.

Exhaust temperature is one of the most important factors for catalyst operation. Carbon monoxide, aldehydes and longer chain hydrocarbons can be reduced by oxidation catalysts with very high efficiencies. Ethane and methane, being more stable compounds, are more challenging requiring higher temperatures to be able to oxide. In present study, the main HC components found in the NG engine exhaust were methane, ethane, propane and ethylene.

Lowest hydrocarbon levels were measured at 100% engine load (see figure 38). The hydrocarbon levels increased with decreasing engine load. The catalyst efficiency to oxide hydrocarbons was also found to increase with the engine load decrease meaning that the highest reductions were recorded at low loads where also the engine out hydrocarbon levels were highest. Also, the exhaust gas temperature rises with decreasing engine load (from 100% to 20%, see Table 6) which is expected to enhance the oxidation reactions.

No methane oxidation was found to occur at any of the load modes (Figure 39 show some reduction percent but this is most probably due to the variations in the natural gas methane levels as well as measurement accuracy). The low exhaust temperatures as well as the catalyst chemistry, most probably, are reasons for the zero level methane oxidation. The catalyst was not designed to oxidize methane. However, some ethane reductions (0-60%) were recorded.

Results – particle emissions

Particle mass measurements according to ISO 8178 were done at engines loads of 100% and 10% (with the two different adjustments). Highest PM levels were found at 10% load and also the PM decrease with the catalyst at 10% load was found to be remarkable. This indicates that most of the PM mass is some volatiles the catalyst is being able to oxidize at the exhaust temperature near 400°C.

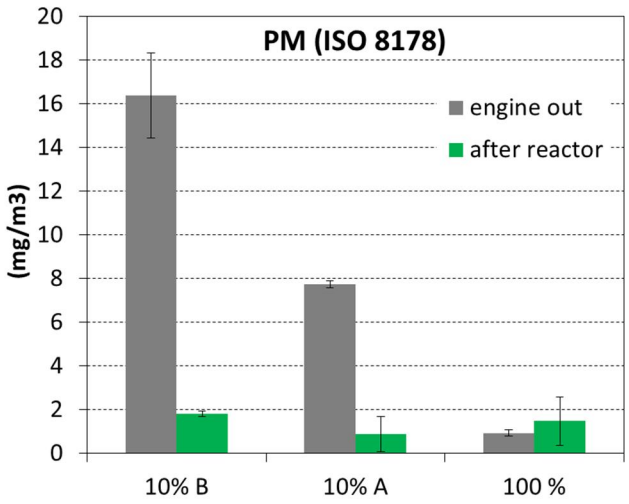

Figure 40 PM measured upstream and downstream of the catalyst reactor.

Figures 41 and 42 present the particle number size distributions derived from the two aerosol instruments in log-log scale. The engine load runs from 10% to 100% from left to right in the figures. The upper graphs represent the situation without exhaust after-treatment while the lower ones show the measured particle number distributions after the reactor. The particle diameter measured by ELPI is the aerodynamic diameter whereas the Nano-SMPS measures the mobility diameter. This must be remembered when interpreting the figures.

Nanoparticles (<100 nm) dominated the particle size distribution and in some cases, majority of the particle had a diameter even below 10 nm. The size distribution peak diameter was, however, at tens of nanometers at the lowest engine loads (10-50%) in the engine out situation. Nano-SMPS observed a particle size distribution with one or two modes depending on the particle concentration and size on the first particle mode. Because of the size range of the instrument, the second particle mode was not captured totally by Nano-SMPS. However, ELPI size distributions confirmed the existence of another particle mode on larger particle sizes (above 10-70 nm). The aerodynamic median diameter of the second particle mode lay around 100-200 nm.

The shape of the particle number size distributions in Figure 42 where the effect of engine adjustment is analyzed resembles the ones in Figure 4. Here, however, the shape at the load 10% B (the same as the 10% in Figure 41) after the reactor can be described as trimodal: one particle size mode below 10 nm, one above 50 nm and one in between. A similar shape can also be seen in Figure 41 at load 100% with exhaust after-treatment, although not this clearly. The existence of a third particle size mode appears to depend on various factors. The same engine situation (same after-treatment, same engine load) did not always generate the similar shape of a particle size distribution: In Figure 41 and in Figure 42 after reactor, 100% graphs were measured on different days, i.e. on a different catalyst usage and engine usage history. On one day a particle mode with diameter below 10 nm formed (Figure 41) and on another day it did not form (Figure 42). This is most likely due to a longer engine operation time when the particle size distributions in figure 42 were measured, resulting in a more stable engine and thus lower formation of volatile particles.

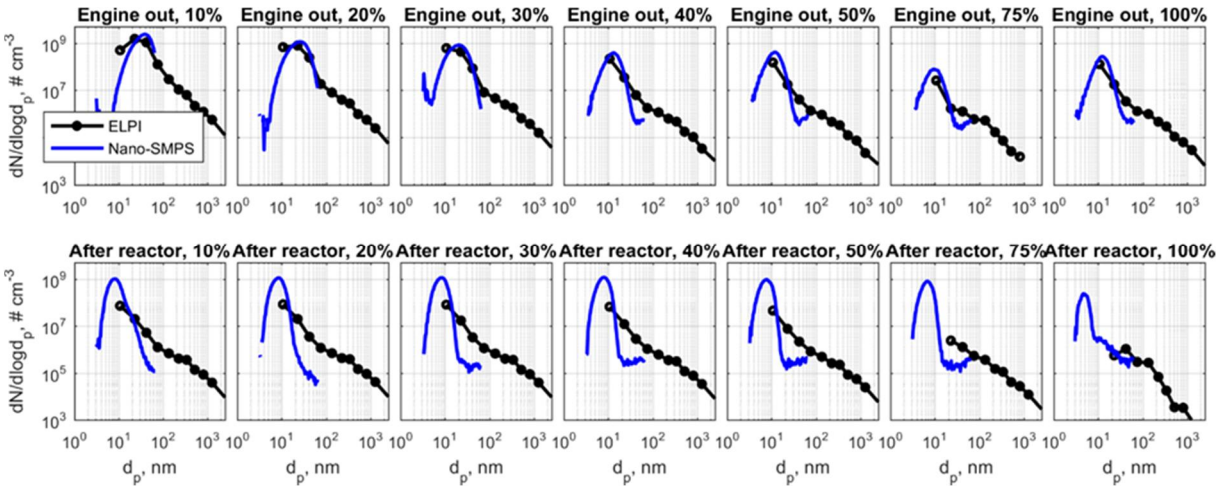

Figure 41 Particle size distributions.

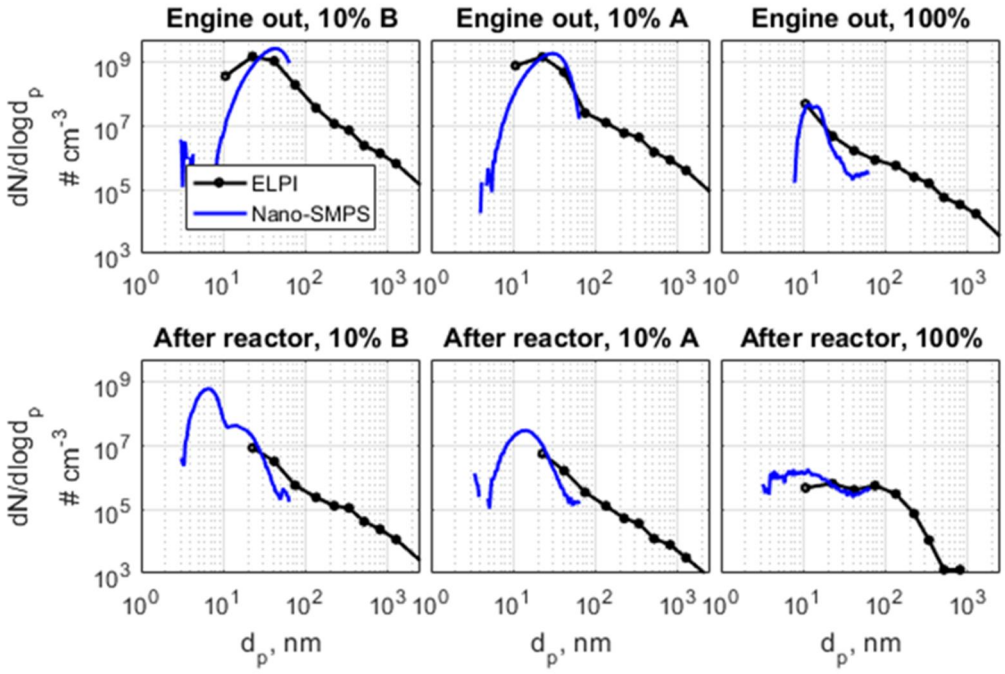

Figure 42 Particle Size distributions.

A log-normal unimodal size distribution has been fitted in the Nano-SMPS number size distribution measurement data in Figure 41. The count median diameters of the fitted size distribution curves are plotted in Figure 43 a) at all the seven engine loads without and with exhaust after-treatment. Without exhaust after-treatment, the particle median diameter decreased from 36 to 9.5 nm when the engine load increased. The smallest particles were emitted at the engine load 75% and the largest at the lowest engine load 10%. Also with catalytic exhaust after-treatment the largest particles were emitted at the lowest engine loads and the smallest at the highest engine loads but the absolute difference between engine loads were less substantial. The catalytic converter affected the particle sizes clearly: for example, at engine load 10% particle mean diameter was reduced by a factor of 4.5 and at engine load 100% by a factor 2.5.

The engine adjustment had a clear effect on particle formation (Figure 42). The size of the particles in the first particle mode was decreased by approximately 15 nm without exhaust after-treatment. With exhaust after-treatment the effect was even clearer: the particle mode with diameter below 10 nm disappeared at load 10% A. These two situations were measured on the same day, first the load 10% A and then the load 10% B.

The total number concentrations presented in Figures 43 b) and 44 a) have been calculated from Nano-SMPS number size distributions. As can be seen in Figures 41 and 42, this method neglects a part of the particles that have a diameter larger than 65 nm but manages to report the trends taking place e.g. in the shift of the engine load. In Figures 43 b) and 44 a) the number concentration with the largest error due to the disadvantage of the measurement technique has been marked with a red circle. Here the actual total number concentration was higher than the measured one. The total mass concentrations in Figures 43 – 46 have been calculated from ELPI size distributions in range 16.3 nm – 1 µm.

The largest number concentrations formed at the lowest engine loads (Figure 43 b)). This was the most evident at engine loads 10% (same as 10% B), 20% and 30% without any exhaust after-treatment. Note that the particle number concentration would actually be even higher at engine load 10% if the instrument could have captured the whole particle mode. When the catalytic converter was applied, the effect of the engine load on the number concentration of the particle emission was more gradual and the largest number

concentrations were in this case emitted by loads 20-40%. The most problematic engine loads were the ones below 30% in terms of particle number emission. The particle number concentrations were the highest at the lowest engine loads. Positively, the exhaust after-treatment system could best decrease the particle number emission at the low loads, even by a factor of >3.3. Strangely, however, the usage of the exhaust after-treatment increased the particle number emission concentration at loads 40-75%.

Similarly to the number concentration, also the particle mass concentrations were decreased with increasing engine load. Again, the largest emission was emitted at the engine loads 10-30% without exhaust after-treatment. The mass concentration emitted at engine load 10% was 14 times higher than at engine load 100%.

The exhaust after-treatment could efficiently reduce the particle mass emission especially at the low loads, but also at the higher engine loads (Figure 43 c and figure 44 b). The reduction in the particulate mass emission was significant, even by a factor of over 20.

The effect of engine adjustment at 10% load on particle number and mass emissions was significant both without and with exhaust after-treatment (Figure 44). Without a catalyst, the reduction in number concentration was over 20% and in mass concentration approximately 50%. With a catalyst, the number and mass emission were reduced by a factor of 15 and 3, respectively.

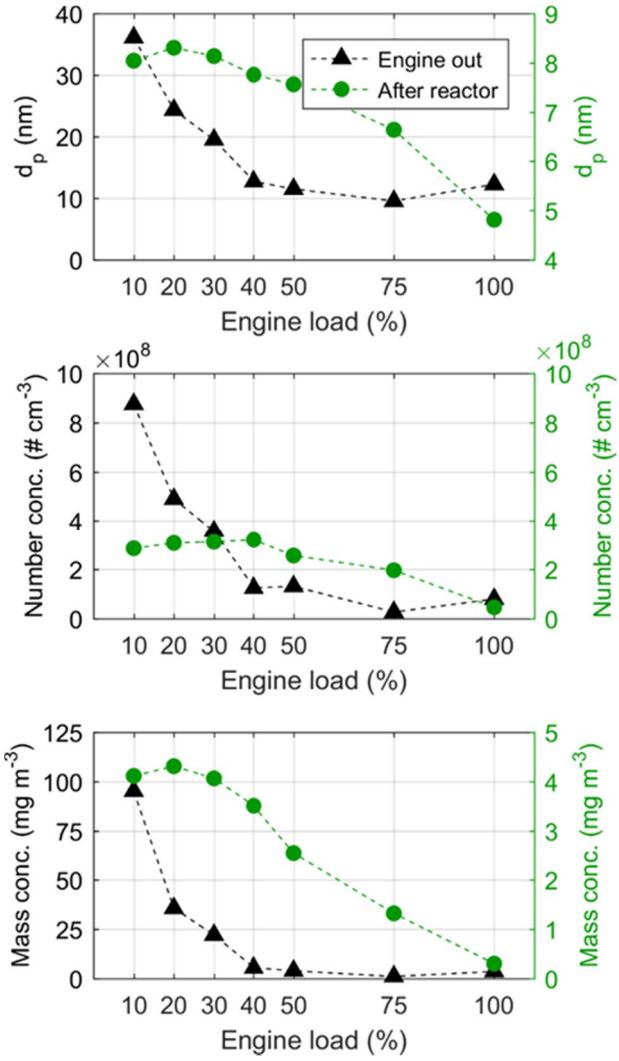

Figure 43 Particle count median diameters, number concentrations and mass concentrations as a function of engine load.

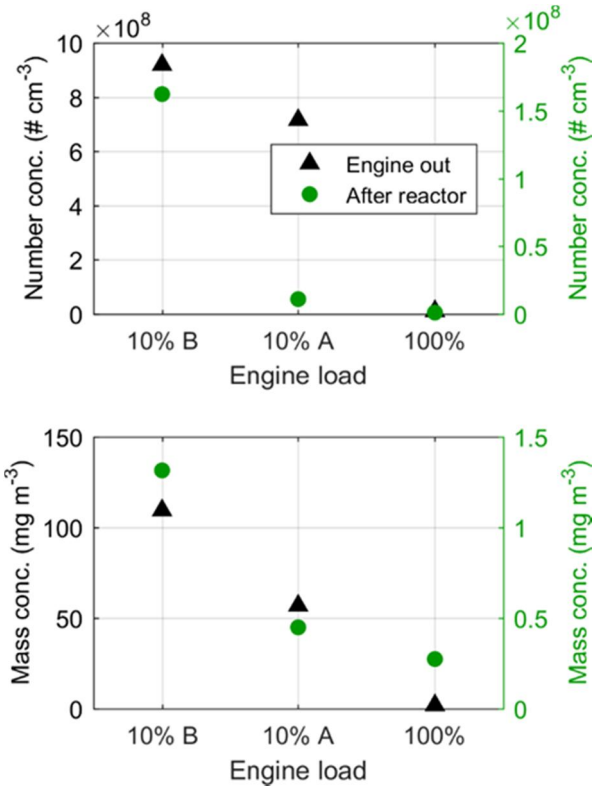

Figure 44 Particle number and mass concentrations as a function of engine load.

In figures 45-48 the particle mass and number concentrations are compared with the particle number concentrations of the non-volatile particles. Figures 45 and 46 present the concentrations without exhaust after-treatment whereas figures 47 and 48 show the fraction of non-volatile particles after the reactor. In general, the particulate matter emitted by the engine was highly volatile both in terms of number and mass. An exception is made by the particles that form after the reactor at engine loads 10% and 100% when the engine was run at a constant load for several hours. It can be concluded that long stable engine operation reduces the formation of volatile particle emissions.

The engine adjustment technology reduced especially the volatile fraction of the particles. Also the steady state operation time of the engine and possibly other variables, such as weather conditions that changed from day to day seem to affect especially the volatile fraction of the particles. This can be seen if particle number concentrations at engine load 100% are compared in figures 47 and 48.

More detailed examination of the non-volatile particles and the thermodenuder treatment will be completed during the on-going process of publishing the real application data. This examination will include a comparison to data from Dekati's High Temperature ELPI+ that sampled directly from the hot, undiluted exhaust.

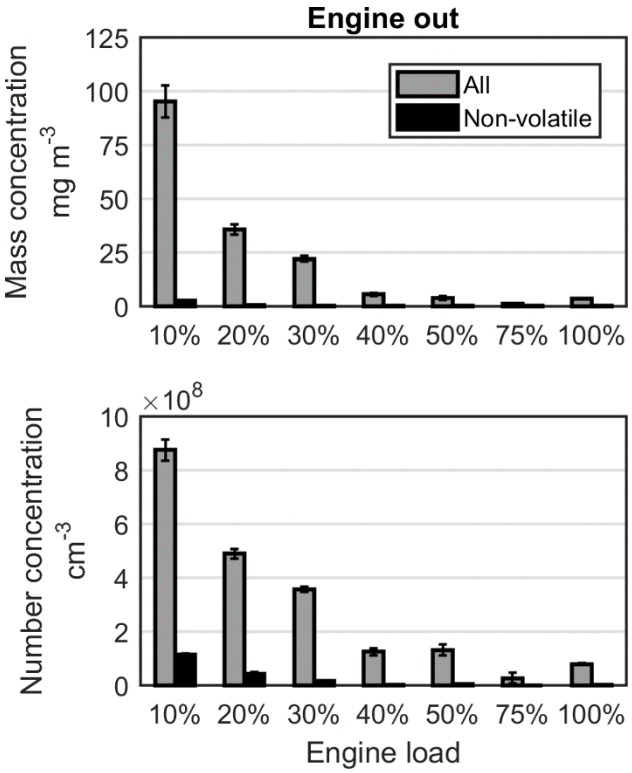

Figure 45 Volatility of engine out particles in terms of particle mass and number concentration.

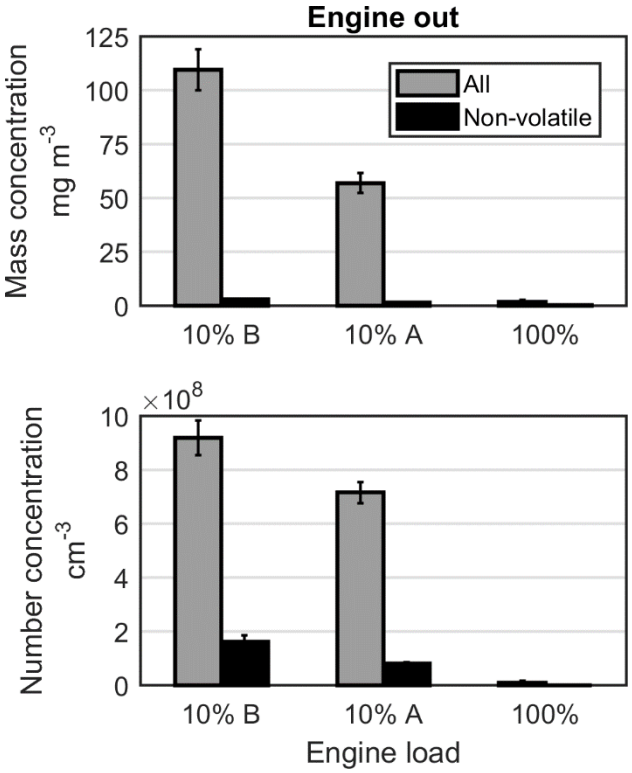

Figure 46 Volatility of engine out particles in terms of particle mass and number concentration. Effect of engine adjustment at 10% load and long engine operation.

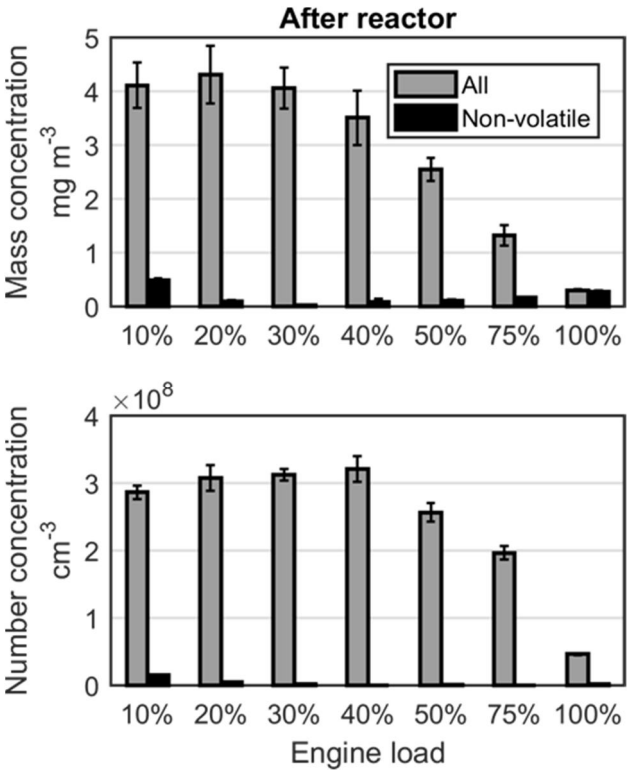

Figure 47 Volatility of particles formed after the catalyst reactor in terms of particle mass and number concentration.

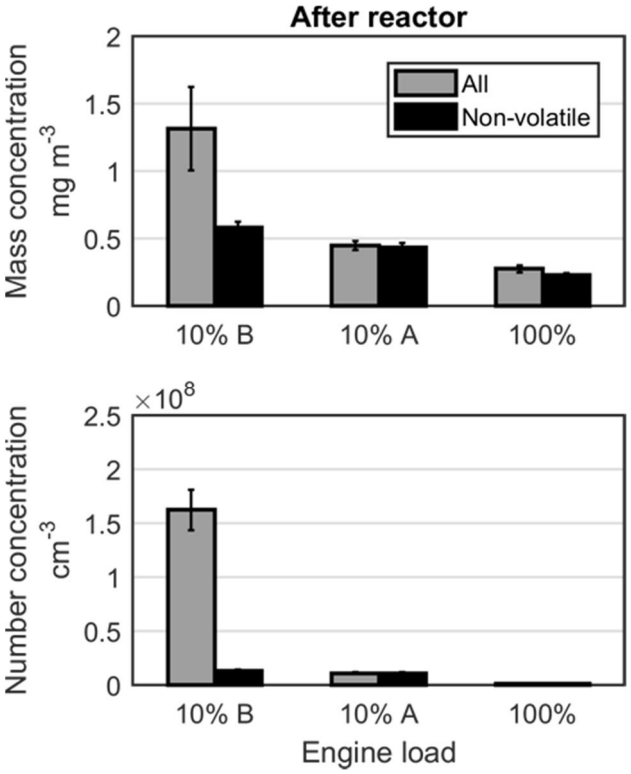

Figure 48 Volatility of particles formed after the catalyst reactor in terms of particle mass and number concentration. Effect of engine adjustment at 10% load and long engine operation.

Main findings of task 4

Results indicate the utilized catalyst reactor was effective technique to decrease the NO_x as well as to decrease CO and aldehydes.

The engine out results showed similar hydrocarbon composition to that of the fuel i.e. natural gas, methane being the main HC species. The engine load was found to have a significant effect on the emission levels. Highest hydrocarbon levels were measured at the lowest load mode of 10%.

Both the exhaust after-treatment and engine load had a significant impact on the particle number and mass emission.The largest mass and number concentrations formed at the lowest engine loads. Positively, the exhaust after-treatment system could best decrease the particle number emission at the low loads, even by a factor of >3.3. Strangely, however, the usage of the exhaust after-treatment increased the particle number emission concentration at loads 40-75%.

A publication related to task 4 is under preparation: *Alanen & Lehtoranta et al. 'Emission formation and reduction on a gas engine power plant with catalysts in use' under preparation – to be submitted 2017*

Task 5 - Instrument tests and calibrations

Target: to test instrument prototypes and new measurement methods at NG engine test facilities, including comparison to commercial instruments and research devices and comprehensive calibration of the selected instruments / prototypes

Particle concentrator

Particle concentrator was tested in the 2nd measurement campaign (task 3) with the SP-AMS. In an ideal case the particle concentrator increases the instrument performance in two ways. It enables shorter detection or integration time, and new compounds become detectable when the particulate mass available for the analysis increases. Theoretically particle concentrator can increase particle concentration by a factor of 25. It is beneficial for the detection of e.g. metals and other elements in the particles. Particle concentrator tested in this project was built at FMI but it was similar to that of Geller et al. (2005; m-VACES). Originally particle concentrators were designed to be used in ambient air. Therefore the aim of this task was to investigate the benefits of using a particle concentrator in gas engine emissions.

The concentrations of selected elements with and without the concentrator are show in Figure 49 for modes 1 and 4 (engine out). Particle concentrator clearly increased the concentrations of all elements, however, the enrichment factor varied between the elements. For mode 1 the largest enrichment ratio was obtained for copper (~10) whereas for mode 4 the largest ratio was measured for zirconium (~14). All the enrichment ratios were smaller than the theoretical ratio of ~25. That was probably due to higher sample temperature in gas engine emission measurement than in ambient air. The growth of particles in the concentration is based on the temperature difference between sample air, (water) saturator and cooling tube (condenser). In order to the concentrator to operate acceptably the temperature of the saturator needs to be 5–10 °C higher than sample temperature. The temperature required by the saturator in the gas engine tests was difficult to achieve with the current device.

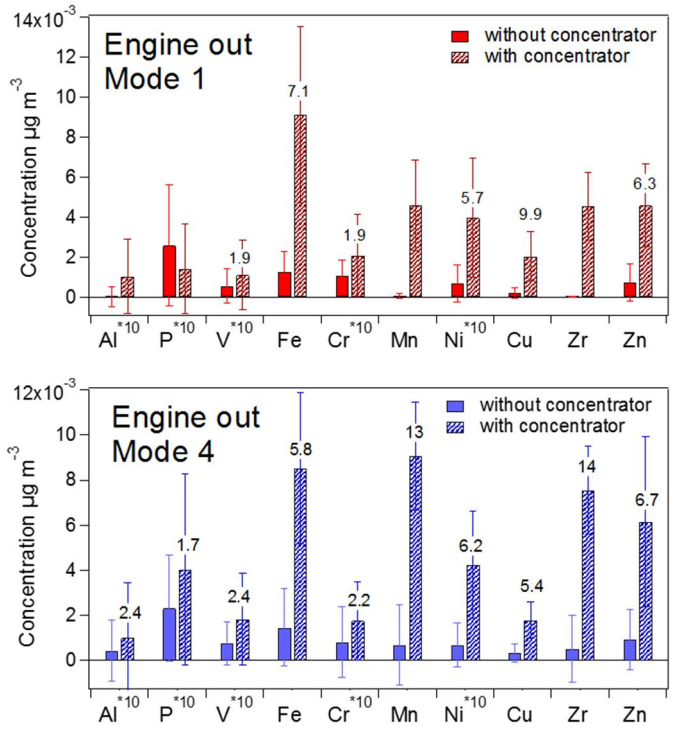

Figure 49. Concentrations of selected elements with and without the particle concentrator. Note that Al, P, V, Cr and Ni concentrations were divided by a factor of 10. Enrichment ratios are given by numbers above the bars.

PSM calibration with silver particles

In exhaust measurements, the particle number size distributions derived from different instruments are wanted to compare which requires overlapping particle size ranges. For that reason, a new calibration for PSM was done on a wider particle size range than before. The calibration has been presented in Alanen et al. (2015).

Calibration of PSM size distribution was performed using silver particles generated by an evaporation-condensation method in a tube furnace. Nitrogen was used as a carrier gas. A small corona charger was used to charge the particles and positively charged particles with sizes starting from 1.3 nm were selected by DMA 3085 (TSI Inc.). The saturator flow of PSM was varied, which changed the growth efficiency of the particles and therefore the detection efficiency of the PSM-CPC combination that was used for measuring the concentration of the particles. The detection efficiency was calculated by first comparing the concentrations measured with each saturator flow with the concentrations with saturator flow 1 lpm and finally comparing the concentrations with the saturator flow 1 lpm with the detection efficiency curve for silver particles with positive electric charge published by Kangasluoma et al. (2013). The calibration results are shown in Figure 49.

Presumably, silver particles do not have exactly the same density and mobility as natural gas engine exhaust particles. Also particle growth with condensing diethylene glycol (DEG, working fluid used in PSM) is material dependent; silver particles were the least prone to grow with condensation of DEG amongst ammonium sulfate, sodium chloride, tungsten oxide and silver in the study of Kangasluoma et al. (2013). The calibration made with silver particles gives an idea in what size range the smallest particles are and provides an opportunity to gain overlapping PSM and Nano-SMPS size distributions.

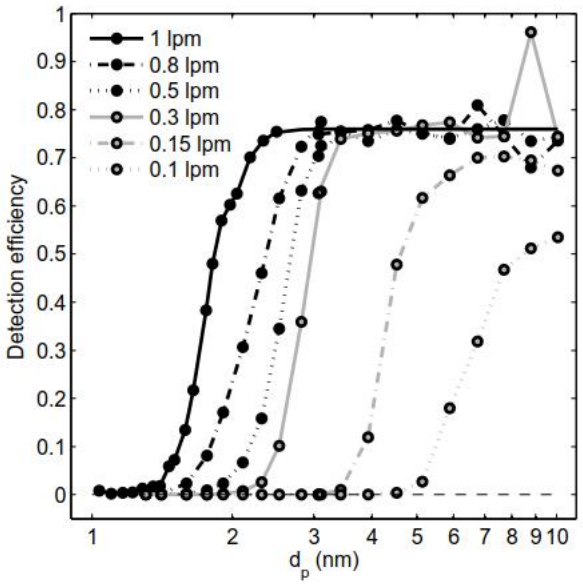

Figure 50 PSM detection efficiency of as a function of particle mobility diameter and PSM saturation flow.

Other activities in instrument testing

Experimental campaigns of the CENGE project were planned and conducted so that their results were able to be utilized also in the measurement method development, also from other aspects than the particle concentrator tests and PSM calibrations described above. The most significant activities and outcomes have been

1) tests for particle size distribution measurement for high temperature exhaust aerosol with relatively low particle concentrations (Niemelä et al. 2015),

2) studies focused on the electrical charging levels of combustion aerosol particles (see e.g. Alanen et al. 2015),

3) laboratory tests for the system coupling the electrical measurement of aerosol particles with conventional filter based particle measurement (Niemelä et al., 2016) and

4) first exhaust studies conducted with a new prototype of oxidation flow reactor for measuring secondary aerosol formation of rapidly changing emission sources. The structure and the functioning of the reactor was published by Simonen et al. (2017), without the data from CENGE project. The secondary aerosol studies from CENGE project has been published by Alanen et al. (2017), based on the use of commercial Potential Aerosol Mass (PAM) reactor.

Main findings of task 5

Low exhaust particle concentrations and small particle sizes require new instrumentation and optimization of the measurement methods. In this project particles were measured from undiluted exhaust using High-Temperature ELPI+, the measured particle size range was expanded down to 1 nm using PSM, and lower dilution ratios than conventionally were applied.

Particle concentrator can be beneficial in gas engine emission measurements but it needs some modification for the saturator unit (new temperature control and saturator material)

Publications related to task 5:

Alanen, J.; Saukko, E.; Lehtoranta, K.; Murtonen, T.; Timonen, H.; Hillamo, R.; Karjalainen, P.; Kuuluvainen, H.; Harra, J.; Keskinen, J.; Rönkkö, T. The formation and physical properties of the particle emissions from a natural gas engine. Fuel 2015, 162, 155-161.

Alanen, J., Simonen, P., Saarikoski, S., Timonen, H., Saukko, E., Hillamo, R., Lehtoranta, K., Keskinen, J., Rönkkö, T. Primary and secondary particle formation and volatility of natural gas engine exhaust. Submitted 2017 in Atmospheric Chemistry and Physics.

Niemelä V., Lamminen E., Lehtoranta K., Rönkkö T. High temperature aerosol measurement – an alternative to dilution approach, 25th CRC REAL WORLD EMISSIONS WORKSHOP, 2015.

Niemelä, V., et al. Gravimetric PM filter holder with real-time particle concentration measurement, 26th CRC REAL WORLD EMISSIONS WORKSHOP, 2016.

Conclusions

The growing trend in the use of natural gas (and also biogas) as energy source enhances the sustainable use of natural resources and can lead to lower CO_2 levels. However, gas combustion is not emission-free. Emissions such as hydrocarbons, especially methane, and formaldehyde, NO_x and particles, all known to have effects on the environment and on human health are found from natural gas exhausts. In the present study, we made a comprehensive emission study from a natural gas engine. Both gaseous sand particle emissions were measured with a wide range of instruments. As expected, high levels of hydrocarbons and carbon monoxide were measured. The major HC component was methane, other components being ethane, propane and ethylene. The portions of methane, ethane and propane of the total HC emissions were similar to the ones in the utilized fuel (i.e. natural gas). The particle mass level was found to be low. However, significant amount of nanoparticles was found in the NG engine exhaust. It was concluded, that the origin of these particles was the combustion chamber or its vicinity while the natural gas and/or lubricating oil originated hydrocarbons and sulphur compounds could magnify the already existing particles in dilution and cooling process, where also new particle formation could happen

In order to deal with the more stringent emission legislation, after-treatment systems, such as catalysts, are increasingly utilized in natural gas applications. In present study, emissions were investigated both upstream and downstream of catalyst systems in order to determine the effects of the catalysts on different emission components. Several different catalysts were utilized, including SCRs, oxidation catalysts, a methane oxidation catalyst (still under development) and combinations of those.

Studies were done with a unique engine research facility developed in the project. By this research facility the emission matrix of a power plant NG engine was mimicked. In addition, the exhaust flow and temperature as well as the exhaust gas composition were modifiable. All these features are seen very relevant in catalyst studies. In addition to experimental studies with this facility one measurement campaign was conducted in a real application power plant gas engine.

The SCR was found to be effective in reducing NO_x. In the present study, the SCR was utilized in two different ways: as a separate catalyst reactor downstream or upstream of an oxidation catalyst and as integrated into an oxidation catalyst. For the integrated system, the oxidation reactions and NO_x reduction reactions were suggested to be competing with each other, resulting in lower NO_x efficiencies at high temperatures. This might imply limitations for utilization; however, this greatly depends on the required NO_x reduction as well as on the possibilities to further optimize the behaviour in different temperature windows. In real applications with, e.g. limited spaces and the need to control the expenses of the catalyst systems, this kind of system can be more attractive compared to two separate catalysts.

Exhaust temperature is one of the most important factors for catalyst operation. Carbon monoxide, aldehydes and longer chain hydrocarbons (non-methane non-ethane) can be reduced by (conventional) oxidation catalysts with very high efficiencies. Short chain hydrocarbons (methane, ethane) are stable compounds requiring higher temperatures to be able to oxidize. With all the oxidation catalyst of present study, very good CO and HCHO reductions were measured, while the propane and ethane oxidation depended greatly on the catalyst and the temperature. To decrease methane a highly active catalyst is needed. The results indicated that the oxidation catalyst developed for methane oxidation can reach methane conversion levels higher than 50% in real natural gas engine exhaust gas applications if the temperature is high enough and the catalyst sizing is correct. However, further studies are needed to solve the long-term performance and the deactivation by sulphur.

Unburned methane is an undesired side product of the natural gas engine combustion. Methane has 28 times higher global warming potential (GWP100) than the CO_2 (Myhre et al. 2013). The lower CO_2 levels resulting from the utilization of natural gas compared to e.g. diesel oil is good for the climate but at the same time methane emission control is important not to compromise the climate benefit gained from the CO_2 decrease. Further development of the oxidation catalysts might be one way to control these methane emissions.

Catalysts and exhaust temperature were found to have a clear effect on particle emissions. At all measurement campaigns catalysts were found to decrease the emissions of particulate matter total mass. However, according to the gained measurement results, nanoparticle number concentrations were increased by a catalyst combined with high exhaust temperatures. At the first catalyst campaign, the behaviour was connected to oxidation of sulphur compounds and generation of sulphuric acid and sulphates. At the second catalyst campaign, by contrast, the increase in particle emission at higher catalyst temperatures was due to an increase in organics. Both the number concentration of the engine out nanoparticles and the PM mass at the second catalyst campaign were significantly lower than at all the previous measurements at the same engine and fuel. The difference between the particulate matter emissions at the campaigns could be explained by lubricating oil: with the commercial lubricating oil the particle emission was lower than with the other oil. However, further studies are needed to confirm and investigate the role of lubricating oil in the nanoparticle formation in more detail. This might also be one more relevant issue in the future, with the growing environmental and human health concerns of (nano) particle emissions.

In addition to primary particle emissions, secondary emission was studied utilizing a potential aerosol mass (PAM) chamber to simulate the aging process of the natural gas engine exhaust in the atmosphere. The mass of total aged particles, i.e. particle mass measured downstream the PAM chamber, was found to be 6-170 times as high as the mass of the emitted primary exhaust particles. The total aged particles consisted mainly of nitrate, organic matter, sulphate and ammonium, the fractions depending on exhaust after-treatment and used engine parameters.

Relatively low particle emissions in engine exhaust can cause even significant challenges for reliable particle emission measurement. Based on the research made in the CENGE project, these challenges can be solved by accurate calibration of instruments, by expanding the measured particle size range, by measuring particle concentrations and other parameters directly from undiluted exhaust, or by the optimizing the exhaust sampling system.

Publications of the project

Journal articles

Alanen, J.; Saukko, E.; Lehtoranta, K.; Murtonen, T.; Timonen, H.; Hillamo, R.; Karjalainen, P.; Kuuluvainen, H.; Harra, J.; Keskinen, J.; Rönkkö, T. The formation and physical properties of the particle emissions from a natural gas engine. Fuel 2015, 162, 155-161.

Murtonen T., Lehtoranta K., Korhonen S., Vesala H., Koponen P. Test facility for catalyst studies utilizing small NG engine. CIMAC Paper 107, 2016.

Lehtoranta K., Murtonen T., Vesala H., Koponen P., Alanen J., Simonen P., Rönkkö T., Timonen H., Saarikoski S., Maunula T., Kallinen K., Korhonen S. Natural gas engine emission reduction by catalysts. Emiss. Control Sci. Technol. 2016, 1-11.

Alanen, J., Simonen, P., Saarikoski, S., Timonen, H., Saukko, E., Hillamo, R., Lehtoranta, K., Keskinen, J., Rönkkö, T. Primary and secondary particle formation and volatility of natural gas engine exhaust. *Submitted 2017 in Atmospheric Chemistry and Physics.*

Saarikoski S., Alanen J., Timonen H., Simonen P., Murtonen T., Vesala H., Rönkkö T., Aurela M., Maunula T., Kallinen K., Korhonen S. and Lehtoranta K. Characterization of natural gas engine emission by aerosol mass spectrometer. *To be submitted 2017*

Alanen & Lehtoranta et al. 'Emission formation and reduction on a gas engine power plant with catalysts in use' *under preparation – to be submitted 2017*

Master's thesis

Jenni Alanen: Kaasumoottorin pakokaasun pienhiukkasten fysikaaliset ominaisuudet. Diplomityö 2014

Conference presentations

Alanen J., Saukko E., Lehtoranta K., Timonen H., Keskinen J. and Rönkkö T. 'Characteristics and formation of natural gas engine exhaust nanoparticles' Aerosol Technology 2015 June 15th to 17th, Tampere.

Niemelä V., Kannosto J., Lehtoranta K., Rönkkö T., Alanen J., Ukkonen A.'High temperature sample and low particle concentration – challenge for measurements' Aerosol Technology 2015 June 15th to 17th, Tampere

Niemelä V., Lamminen E., Lehtoranta K., Rönkkö T. 'High temperature aerosol measurement – an alternative to dilution approach' 25th CRC REAL WORLD EMISSIONS WORKSHOP, 2015.

S. Saarikoski, H. Timonen, T. Murtonen, H. Vesala, J. Alanen, T. Rönkkö, R. Hillamo, T. Maunula, K. Kallinen, S. Korhonen and K. Lehtoranta. Characterization of natural gas engine emission by aerosol mass spectrometer, EAC 2016 Tours, France

Rönkkö T., Alanen J., Saukko E., Lehtoranta K., Murtonen T., Timonen H., Hillamo R., Karjalainen P., Kuuluvainen H., Harra J., Keskinen J. Nanoparticles in natural gas engine exhaust, 5th International Exhaust Emissions Symposium 2016, Poland

Lehtoranta K., Alanen J., Rönkkö T., Simonen P., Murtonen T., Vesala H., Saarikoski S., Timonen H., Maunula T., Kallinen K., Korhonen S. Particle emissions from a natural gas engine with and without a catalyst, ETH Nanoparticles 2016

Rönkkö T., Alanen J., Saukko E., Lehtoranta K., Saarikoski S., Karjalainen P., Simonen P., Murtonen T., Timonen H., Teinilä K., Kuuluvainen H., Hillamo R., Keskinen J. Nanoparticles in natural gas engine exhaust, ETH Nanoparticles 2017

Lehtoranta K., Murtonen T., Vesala H., Koponen P., Alanen J., Kuittinen N., Simonen P., Rönkkö T., Saarikoski S., Timonen H., Maunula T., Kallinen K., Korhonen S. Controlling emissions of natural gas engines. A&WMA's 110th Annual Conference, June 5-8, 2017

Other publications

Lehtoranta, K. CENGE - Controlling Emissions of Natural Gas Engines. Polttomoottori- ja turbotekniikan seminaari 15.5.2014

IL:n Tiedeuutinen: Kaasumoottorin tuottamat pienhiukkaset kooltaan pieniä muihin polttoaineisiin verrattuna. 2015.

Alanen, J. Measurements of natural gas engine exhaust nanoparticles by PSM. Air Ions, Clusters and Atmospheric Aerosols Workshop 2016 August 23rd to 25th, Hyytiälä.

Rönkkö, T. CENGE pureutui kaasumoottoreiden päästöihin, Ilmansuojeluyhdistys ry:n jäsenlehti 2017, 1, 18-21.

IL:n Tiedeuutinen: Katalyytit vähensivät maakaasumoottorin kaasu- ja hiukkaspäästöjä. 2017.

In addition: CENGE methane catalyst results informed to IEA AMF programme, Annex 51: Methane Emission Control

References

Abdelaal, M.M., Hegab, A.H.: Combustion and emissions characteristics of a natural gas-fueled diesel engine with EGR. Energy Convers. Manag. 64, 301–312 (2012)

Alanen, J., Saukko, E., Lehtoranta, K., Murtonen, T., Timonen, H., Hillamo, R., Karjalainen, P., Kuuluvainen, H., Harra, J., Keskinen, J., Rönkkö, T.: The formation and physical properties of the particle emissions from a natural gas engine. Fuel 162, 155–161 (2015)

Arnold, F., Pirjola, L., Rönkkö, T., Reichl, U., Schlager, H., Lähde, T., Heikkilä, J. and Keskinen, J.: First online measurements of sulfuric acid gas in modern heavy-duty diesel engine exhaust: Implications for nanoparticle formation, Environ. Sci. Technol., 46(20), 11227–11234 (2012).

Canagaratna, M.R., Jayne, J.T., Ghertner, D.A., Herndon, S., Shi, Q., Jimenez, J.L., Silva, P.J., Williams, P., Lanni, T., Drewnick, F., Demerjian, K.L., Kolb, C.E.,Worsnop, D.R.: Chase studies of particulate emissions from in-use NewYork City vehicles. Aerosol Sci. Technol. 38, 555–573 (2004).

Chirico, R., Prevot, A.S.H., DeCarlo, P.F., Heringa, M.F., Richter, R., Weingartner, E., Baltensperger, U.: Aerosol and trace gas vehicle emission factors measured in a tunnel using an aerosol mass spectrometer and other on-line instrumentation. Atmos. Environ. 45, 2182–2192 (2011).

Cho, H. M. and He, B. Q.: Spark ignition natural gas engines-A review, Energy Convers. Manag., 48(2), 608–618 (2007).

Forzatti, P., Lietti, L.: Recent advances in De-NOxing catalysis for stationary applications. Heterog. Chem. Rev. 3, 33–51 (1996)

Geller, G. D., Biswas, S., Fine, P. M., and Sioutas, C.: A new compact aerosol concentrator for use in conjunction with low flow-rate continuous aerosol instrumentation, J. Aerosol Sci., 36, 1006–1022, 2005.

Hesterberg, T.W., Lapin, C.A., Bunn,W.B.: A comparison of emissions from vehicles fuelled with diesel or compressed natural gas. Environ. Sci. Technol. 42, 6437–6445 (2008).

Jayaratne, E. R., Ristovski, Z. D., Meyer, N. and Morawska, L.: Particle and gaseous emissions from compressed natural gas and ultralow sulphur diesel-fuelled buses at four steady engine loads, Sci. Total Environ., 407(8), 2845–2852 (2009).

J. Kangasluoma, H. Junninen, K. Lehtipalo, J. Mikkilä, J. Vanhanen, M. Attoui, M. Sipilä, D. Worsnop, M. Kulmala and T. Petäjä, Remarks on Ion Generation for CPC Detection Efficiency Studies in Sub-3-nm Size Range, Aerosol Science and Technology 47 (2013) 556–563.

Kittelson, D.B.,Watts,W.F., Johnson, J.P., Thorne, C., Higham, C., Payne, M., Goodier, S.,Warrens, C., Preston, H., Zink, U., Pickles, D., Goersmann, C., Twigg,M.V.,Walker, A.P., Boddy, R.: Effect of fuel and lube oil sulfur on the performance of a diesel exhaust gas continuously regenerating trap. Environ. Sci. Technol. 42, 9276– 9282 (2008).

Koebel,M., Strutz, E.O.: Thermal and hydrolytic decomposition of urea for automotive selective catalytic reduction systems: thermochemical and practical aspects. Ind. Eng. Chem. Res. 42, 2093– 2100 (2003).

Lambert, J.K., Kazi, M.S., Farrauto, R.J.: Palladium catalyst performance for methane emissions abatement from lean burn natural gas vehicles. Appl. Catal. B Environ. 14, 211 223 (1997).

Lehtoranta, K., Vesala, H., Koponen, P., Korhonen, S.: Selective catalytic reduction operation with heavy fuel oil: NOx and NH3, and particle emissions. Environ. Sci. Technol. 49, 4735–4741 (2015).

Lehtoranta K., Murtonen T., Vesala H., Koponen P., Alanen J., Simonen P., Rönkkö T., Timonen H., Saarikoski S., Maunula T., Kallinen K., Korhonen S. Natural gas engine emission reduction by catalysts. Emiss. Control Sci. Technol. 2016, 1-11.

Lietti, L., Nova, I., Forzatti, P.: Selective catalytic reduction of NO by NH3 over TiO2-supported V2O5-WO3 and V2O5-MoO3 catalysts. Top. Catal. 11, 111–122 (2000)

Liu, J., Yang, F., Wang, H., Ouyang, M., Hao, S.: Effects of pilot fuel quantity on the emissions characteristics of a CNG/diesel dual fuel engine with optimized pilot injection timing. Appl. Energy 110, 201–206 (2013)

Lähde, T., Rönkkö, T., Virtanen, A., Schuck, T., Pirjola, L., Hämeri, K., Kulmala, M., Arnold, F., Rothe, D. and Keskinen, J.: Heavy Duty Diesel Engine Exhaust Aerosol Particle and Ion Measurements, Environ. Sci. Technol., 43(1), 163–168 (2009).

Majewski, W.A., Khair, M.K.: Diesel emissions and their control. SAE International, Warrendale (2006)

Maricq, M.M., Chase, R.E., Xu, N., Laing, P.M.: The effects of the bcatalytic converter and fuel sulfur level on motor vehicle particulate matter emissions: light duty diesel vehicles. Environ. Sci. Technol. 36, 283–289 (2002)

Mitchell, C.E., Olsen, D.B.: Formaldehyde formation in large bore natural gas engines part 1: formation mechanisms. J. Eng. Gas Turbines Power 122, 603–610 (2000)

Murtonen, T., Lehtoranta, K., Korhonen, S., Vesala, H., Koponen, P.: Imitating emission matrix of large natural gas engine opens new possibilities for catalyst studies in engine laboratory. CIMAC Pap. pp. 107 (2016)

Olin, M., Rönkkö, T., Maso, M. D. and Olin, C. M.: CFD modeling of a vehicle exhaust laboratory sampling system: sulfur-driven nucleation and growth in diluting diesel exhaust, Atmos. Chem. Phys., 15, 5305–5323 (2015).

Olsen, D.B., Mitchell, C.E.: Formaldehyde formation in large bore natural gas engines part 2: factors affectingmeasured CH2O. J. Eng. Gas Turbines Power 122, 611–616 (2000)

Olsen, D.B., Kohls,M., Arney, G.: Impact of oxidation catalysts on exhaust NO2/NOx ratio from lean-burn natural gas engines. J. Air Waste Manage. Assoc. 60, 867–874 (2010)Ottinger et al. (2015)

Pirjola, L., Karl, M., Rönkkö, T., Arnold, F.: Model studies of volatile diesel exhaust particle formation: are organic vapours involved in nucleation and growth? Atmos. Chem. Phys. 15, 10435– 10452 (2015)

Pope, C. A., Dockery, D. W., Chow, J. C., Watson, J. G., Mauderly, J. L., Costa, D. L., Wyzga, R. E., Vedal, S., Hidy, G. M., Altshuler, S. L., Marrack, D., Heuss, J. M., Wolff, G. T., Arden Pope III, C. and Dockery, D. W.: Health Effects of Fine Particulate Air Pollution: Lines that Connect, J. Air Waste Manage. Assoc., 56(10), 1368–1380 (2006).

Ristovski, Z. D., Morawska, R. L., Hitchins, J., Thomas, S., Greenaway, C. and Gilberts, D.: Particle emissions from compressed natural gas engines, J. Aerosol Sci., 31(4), 403–413, (2000).

Rönkkö, T., Lähde, T., Heikkilä, J., Pirjola, L., Bauschke, U., Arnold, F., Schlager, H., Rothe, D., Yli-Ojanperä, J. and Keskinen, J.: Effects of gaseous sulphuric acid on diesel exhaust nanoparticle formation and characteristics, Environ. Sci. Technol., 47(20), 11882–11889 (2013).

Seinfeld, J. H., & Pandis, S. N. (2006). Atmospheric chemistry and physics: From air pollution to climate change. Hoboken, N.J: J. Wiley.

Simonen, P., Saukko, E., Karjalainen, P., Timonen, H., Bloss, M., Aakko-Saksa, P., Rönkkö, T., Keskinen, J., and Dal Maso, M.: A new oxidation flow reactor for measuring secondary aerosol formation of rapidly changing emission sources, Atmos. Meas. Tech., 10, 1519-1537, doi:10.5194/amt-10-1519-2017, 2017.

Vaaraslahti, K., Virtanen, A., Ristimäki, J., Keskinen, J.: Nucleation mode formation in heavy-duty diesel exhaust with and without a particulate filter. Environ. Sci. Technol. 38, 4884–4890 (2004)

Yim, S.D., Kim, S.K., Baik, J.B., Nam, I.-S., Mok, Y.S., Lee, J.-H., Cho, B.K., Oh, S.H.: Decomposition of urea into NH3 for the SCR process. Ind. Eng. Chem. Res. 43, 4856–4863 (2004)

Appendix

Lubricating oil analysis results

			CENGE Commercial oil	CENGE 5W-30 OIL#2	CENGE 5W-30 OIL#1
ENISO12185	Density	kg/m3	889,7	852,7	852,3
ASTMD5950	Pour point	°C	-9	-45	-45
ENISO3104	Viscosity 40°C	mm2/s	124,7	68,4	70,55
ENISO3104	Viscosity 100°C	mm2/s	13,96	11,95	12,03
ASTMD2270	Viscosity index		110	172,6	168,3
ENISO20846	Sulphur	mg/kg	>8000	1282	1763
CECL-40-93-B	NOACK	wt-%	4,4	10,1	8,7
ASTMD5185	Manganese	mg/l	<0,3	0,6	<0,2
ASTMD5185	Calsium	mg/kg	1200	2580	2640
ASTMD5185	Copper	mg/kg	<0,1	<0,3	<0,3
ASTMD5185	Iron	mg/kg	0,57	0,9	1
ASTMD5185	Magnesium	mg/kg	2,4	7,4	13
ASTMD5185	Molybdenum	mg/kg	0,83	<0,3	<0,3
ASTMD5185	Sodium	mg/kg	<1,0	1,6	3,7
ASTMD5185	Nickel	mg/kg	<0,5	<0,5	<0,3
ASTMD5185	Silicon	mg/kg	8,4	3,7	<0,3
ASTMD5185	Phosphorus	mg/kg	290	720,9	937,5
ASTMD5771	Cloud point	°C		-12	-13,3
ASTMD5185	Cadmium	mg/kg	<0,5	<0,5	<0,5
ASTMD5185	Aluminium	mg/kg	2	3,2	1
ASTMD5185	Lead	mg/kg	<0,6	<0,6	<0,6
ASTMD5185	Tin	mg/kg	<1	<1	<1
ASTMD5185	Vanadium	mg/kg	<0,3	<0,3	<0,3
ASTMD5185	Barium	mg/kg	<0,3	0,5	<0,3
ASTMD5185	Zinc	mg/kg	330	700	920
ASTMD874	Sulphated ash	%	0,452	0,974	1,04